blockade reversed the PAI-1 inhibitor-mediated improved neovascularization and neutrophil recruitment in the peripheral blood and locally within the ischemic tissue/niche. Remarkably, adoptive transfer of ischemic muscle-derived neutrophils derived from PAI-1 inhibitor-treated mice enhanced revascularization. Pharmacologic PAI-1 blockade under ischemic conditions not only increased the absolute number of granulocyte-1 marker (Gr-1$^+$) myeloid cells, but also enhanced their angiogenic performance.

These data provide a fundamental insight into how PAI-1 conditioning of the ischemic niche induces leukocyte influx and controls angiogenesis and suggest that PAI-1 inhibition using small-molecule inhibitors could be a promising cellular target for the treatment of ischemic diseases.

Methods

Animal studies

MMP-9$^{+/+}$ and MMP-9$^{-/-}$ mice and tPA$^{+/+}$ and tPA$^{-/-}$ mice were each used after > 10 back crosses onto a C57BL/6 background. C57BL/6 mice were purchased from SLC. C57BL/6 mice that express GFP under a β-actin promoter were used for transplantation experiments at the age of 6-8 weeks. Animal studies were approved by the animal review board of Juntendo University.

PAI-1 inhibitor

The recently described PAI-1 inhibitor TM5275, 5-chloro-2-((2-(4-(diphenylmethyl) piperazin-1-yl)-2-oxoethoxy acetyl)amino]benzoate, provided by T.M. inhibited PAI-1 activity with a half-maximal inhibition (IC$_{50}$) value of 6.95μM, as measured by assay of tPA-dependent hydrolysis of a peptide substrate. The IC$_{50}$ values of TM5007 and PAI-749 are 5.60, and 8.37μM, respectively.[18] In vitro, TM5275 (up to 100μM does not interfere with other serpin/serine protease systems such as alpha$_1$-antitrypsin/trypsin and alpha$_2$-antiplasmin/plasmin). Therefore, its PAI-1–inhibitory activity appears to be specific. Preincubation of PAI-1 with TM5275 abolishes detection of the covalent PAI-1–tPA complex by SDS-PAGE.[18] Oral administration of 50 mg/kg of TM5275 to mice resulted in a maximum plasma concentration after 1 hour. The highest plasma drug concentration observed was 6.9 mol/L and the terminal phase half-life of the drug was 6.5 hours. No effect of TM5275 on platelet aggregation induced by ADP and collagen was observed 2 hours after oral administration (10 mg/kg).

Study design

The PAI-1 inhibitor was resuspended in 200 μL of 0.5% carboxymethylcellulose (MP Biomedicals) and administered orally (10 mg/kg body weight) daily to mice with or without induction of HL ischemia from days 0-6. Control mice received vehicle (200 μL of 0.5% carboxymethylcellulose). Recombinant tPA (Eizai) resuspended in 150 mL of 0.2% BSA (Sigma-Aldrich) was administered (10 mg/kg body weight) to mice by daily IP injections from days 0-2.[19]

HL model

Mice were anesthetized with pentobarbital sodium (40 mg/kg body weight) that was given intraperitoneally. Briefly, an incision was made in the skin on the medial aspect of the left thigh. The femoral artery was ligated using 4-0 silk sutures (Ethicon) and cut immediately distal to the inguinal ligament and proximal to the popliteal bifurcation site. Changes in blood flow were recorded at days 0, 1, 4, 7, 14, and 21 after the procedure using a laser Doppler perfusion image analyzer (Moor Instruments). Blood was collected via retroorbital bleeding using heparin-coated and plain capillary tubes and WBCs were counted. Plasma and serum samples were stored at −30°C. Mice were killed 1, 5, 15, and 21 days after resection of the femoral artery.

Isolation of Gr-1 cells from muscle tissue after HL ischemia induction

Muscle-derived Gr-1$^+$ cells were isolated from HL-ischemia–induced C57BL/6 mice treated with or without PAI-1 inhibitor on day 5 using MACS. In brief, muscles were excised and cut into small pieces. After excision, tissue pieces were lysed with a buffer containing 20mM Tris-HCl, 5mM EDTA, 1% collagenase II, 2.4 U/mL of Dispase, 1mM PMSF, and 10 μmol pepstatin for 1.5 hours. Gr-1$^+$ and Gr-1$^-$ cells were isolated using the anti–Ly-6G Microbead kit (Miltenyi Biotec). Cell morphology was determined on cytospins after Wright-Giemsa staining.

In vivo blocking experiments

HL-ischemic mice treated with or without the PAI-1 inhibitor (days 0-6) were coinjected intraperitoneally with 10 μg of anti–mouse VEGF-A (AF-493-NA; R&D Systems) or 10 μg of goat specific anti–human FGF-2 (AF-233-NA; R&D Systems) on day 0. Appropriate isotype Ab controls were included.

Transplantation of PAI-1 inhibitor-mobilized Gr-1$^+$ cells

Muscle-derived Gr-1$^+$ cells were isolated from HL-ischemia–induced C57BL/6 donor mice treated with or without PAI-1 inhibitor on day 5 by FACS using a FACSCalibur flow cytometer (BD Biosciences). Gr-1$^+$ cells (5 × 10^4 cells/injection/d) were injected daily intramuscularly into C57BL/6 recipient mice on days 0 and 1 after HL ischemia induction.

Flow cytometry

PBMCs were stained with the following Abs: CD45-FITC (1:200, clone 30-F11; BD Pharmingen), CD11b-APC (1:200, clone M1/70; BD Pharmingen), and Gr-1-PE (1:200, clone RB6-8C5; BD Pharmingen). Cells were analyzed by FACS.

Histological assessment

Ischemic adductor or, if indicated, hamstring (posterior thigh) muscle tissue samples were snap-frozen in liquid nitrogen. Transverse cuts of the whole leg were prepared. Sections were stained with H&E.

Tissue sections were washed, serum blocked, and stained with the first Ab overnight at 4°C. Muscle sections were stained with the anti-CD31 Ab (clone T-2001; BMA Biomedicals) followed by biotin-conjugated goat anti–rat IgG (Vector Laboratories) and FITC-conjugated streptavidin (Alexa Fluor 488; Molecular Probes). In addition, tissues were stained with the primary anti–mouse FGF-2 (clone D0611; Santa Cruz Biotechnology) and FGF-R1 (clone 755639; Abcam) and VEGF-A Abs, followed by a goat anti–rabbit IgG Ab conjugated with Alexa Fluor 488 (Molecular Probes). Muscle sections were also stained with anti–mouse VWF Ab (Dako), followed by Cy3-conjugated streptavidin (Alexa Fluor 594; Molecular Probes) using the M.O.M kit (Vector Laboratories) according to the manufacturer's instructions. Neutrophils were identified using the Gr-1 Ab (clone RB6-8C5; R&D Systems), followed by biotin-conjugated goat anti–rat IgG (Vector Laboratories) and Cy3-conjugated streptavidin (Alexa Fluor 594; Molecular Probes) Abs. Macrophages were identified using the F4/80 Ab (clone A3-1; AbD Serotec), followed by biotin-conjugated goat anti–rat IgG (Vector Laboratories) and Cy3-conjugated streptavidin (Alexa Fluor 594; Molecular Probes) Abs. In addition, tissues were stained with the primary anti–mouse VEGF-A Ab (clone A-20; Santa Cruz Biotechnology), followed by the goat anti–rabbit IgG Ab conjugated with Alexa Fluor 488 (Molecular Probes). Nuclei were counterstained with DAPI (Molecular Probes).

RT-PCR analysis

Total RNA was extracted from the gastrocnemius muscle of HL-ischemic or untreated mice using RNA TRIzol (Invitrogen) according to the manufacturer's directions. Briefly, 25 mg of muscle was immediately immersed in 1 mL of TRIzol reagent. The muscle was homogenized on ice using a homogenizer. The aqueous and organic phases were separated using 200 μL

of chloroform. Total RNA was precipitated using 500 μL of isopropyl alcohol, washed 3 times with 75% ethanol, and redissolved in 24 μL of DEPC-treated H$_2$O. The concentration and purity of the RNA was determined using a UV spectrophotometer by measuring the absorbance at 260 and 280 nm. cDNA was amplified by PCR using the following specific forward and reverse primer pairs: for *uPA*: (5′-GTCCTCTCTGCAACA-GAGTC-3′) and (5′-CTGTGTCTGAGGGTAATGCT-3′); for *tPA*: (5′-GTACTGCTTTGTGGACT-3′) and (5′-TGCTGTTGGTAAGTTGTCTG-3′); for *PAI-1*: (5′-AAAGGACTCTATGGGGAGAA-3′) and (5′-TAGGGAG-GAGGGAGTTAGAC-3′); and for the *b-actin* control: (5′-TGACAGGATG-CAGAAGGAGA-3′) and (5′-GCTGGAAGGTGGACAGTGAG-3′).

ELISA

Plasma and serum samples from PAI-1 inhibitor-treated and untreated mice with HL-ischemia induction were assayed for murine VEGF-A, MMP-9, KitL, G-CSF, PAI-1, and tPA using ELISA kits (R&D Systems, Cell Sciences, and Molecular Innovations).

Western blotting

Muscle tissue extracts were prepared for Western blotting. Briefly, gastroc-nemial muscle tissues were lysed in a buffer containing 20mM Tris-HCl, 5mM EDTA, 1% Triton X-100, 1mM PMSF, and 10μM pepstatin after mashing between 2 glass slides. Whole-muscle lysates were subjected to SDS-PAGE (8%), followed by electroblotting onto a PVDF membrane. Membranes were blocked in 20mM PBS and 0.05% Tween-20 (vol/vol) containing 5% (wt/vol) skim milk powder at room temperature, followed by overnight incubation with the anti–PAI-1 Ab (1:1000; Abcam), and an HRP-conjugated secondary Ab (1:20; Nichirei Biosciences) for 1 hour. Membranes were developed using the ECL Plus system (Amersham Life Sciences).

Reverse fibrin zymography

Reverse fibrin zymography, although similar to fibrin zymography, uses agar gels that contain uPA in addition to fibrinogen and plasminogen to determine unbound/free PAI-1. Protein extracts (50 μg) from normal and ischemic muscle tissues were loaded on an 8% acrylamide gel, and, after SDS-PAGE, the SDS was removed by washing the acrylamide gels with distilled water followed by incubation for 2 hours with a buffer containing 2.5% Triton X-100, 0.05 M/L of Tris-HCl (pH 7.5), and 0.1 M/L of NaCl to renature the enzymes. The gels were then incubated for 12-24 hours at 37°C in buffer containing 0.05 M/L of Tris-HCl (pH 7.5) and 0.01 M/L of CaCl$_2$. After this incubation, the gels were stained for 1 hour with Coomassie blue diluted with 50% methanol and 10% acetic acid and decolorized with buffer containing 25% methanol and 8% acetic acid. No fibrinolysis occurs in the area of the gel where the PAI-1 protein is located, resulting in a visible band. Gels were then photographed.

Fibrin plate assay

Plasma fibrinolytic activity was measured using the modified fibrin plate method. Briefly, blood samples were collected in plain tubes containing 3.2% sodium citrate, mixed at a ratio of 9:1, and centrifuged at 3000*g* for 20 minutes at 4°C. The euglobulin fraction was prepared by acidification of 1:10 diluted plasma to pH 5.9 with 0.25% (vol/vol) glacial acetic acid at 4°C, which was then centrifuged at 500*g* at 4°C for 10 minutes. The supernatant was discarded. The euglobulin precipitate was resuspended in an EDTA-gelatin-barbital buffer (pH 7.8), and 30 mL of each sample were placed in identical depressions in a fibrin-agarose plate. Next, 10 mL of a 1.5 mg/mL bovine fibrinogen solution in Barbitol buffer (50mM sodium barbitol, 90mM NaCl, 1.7mM CaCl$_2$, and 0.7mM MgCl$_2$, pH 7.75) and 10 mL of a 1% agarose solution were brought to 45°C in a water bath, and 10 NIH units of thrombin (250 NIH units/mL) were then added into the agarose solution. The fibrinogen and agarose solutions were mixed in a 140-mm Petri dish and kept at room temperature for 2 hours to form fibrin clots. Enzymes were dissolved and diluted to the appropriate concentration in Barbitol buffer. Each enzyme solution (10 mL) was dropped into a hole preformed on the fibrin plate. The plate was incubated at 37°C for 18 hours.

The zone of lysis on the fibrin plate (fibrinolytic activity) was measured using Area Manager (Ruka International).

Statistical analyses

All data are presented as means ± SEM. Student *t* tests were performed. $P < .05$ was considered significant.

Results

Ischemia is associated with increased expression of PAI-1 in ischemic muscle tissue

Because oxygen deprivation, such as that which occurs during tissue ischemia, can tip the natural anticoagulant/procoagulant balance,[20] in the present study, we investigated whether the fibrinolytic factors are present within ischemic gastrocnemius muscle tissues. An increase in *PAI-1*, *uPA*, and *tPA* mRNA expression, as determined using quantitative PCR (Figure 1A-C), and an increase in PAI-1 protein and activity, as determined by Western blotting and reverse fibrin zymography, respectively (Figure 1D-E), were detected in ischemic muscle tissues from HL ischemia-induced mice compared with nonischemic controls. These results demonstrated that ischemia increased ischemic muscle PAI-1 activity and simultaneously augmented local fibrinolytic activity.

We next evaluated the effects of administration of the PAI-I inhibitor TM5275 on fibrinolytic factor release into the circulation. The PAI-1 inhibitor TM5275 (hereafter referred to as the PAI-I inhibitor) is an effective novel oral drug that inhibits PAI-1 by preventing binding of PAI-1 to tPA.[18] Both active and latent forms of PAI-1 can circulate.[20] PAI-1 inhibits tPA and uPA and PAI-1 is usually present in excess over tPA in plasma. In the present study, PAI-1 inhibitor treatment administered daily from days 0-6 blocked the systemic increase in active PAI-1 in plasma (Figure 1F) and augmented plasma tPA (Figure 1G) and plasmin levels during HL-ischemic recovery (Figure 1H). When the PAI inhibitor treatment was suspended, plasma tPA and plasmin levels returned gradually to baseline levels in 14-21 days. These data indicate that PAI inhibition during ischemic recovery creates a fibrinolytic state.

Pharmacologic targeting of PAI-1 promotes ischemic revascularization and tissue regeneration.

We next determined the consequences of PAI-1 inhibition for tissue regeneration after HL ischemia induction by treating ischemia-induced C57BL6/C mice with the PAI-1 inhibitor or vehicle control. Foot digit necrosis was prevented in PAI-1 inhibitor-treated animals (Figure 1I). The ischemic limb of PAI-1 inhibitor-treated mice displayed faster perfusion recovery, as determined by laser Doppler perfusion image analysis, than vehicle-treated controls (Figure 1I-J). Smaller areas of necrosis were detected in histochemically stained ischemic muscle tissue sections of the lower and upper limb (ie, the gastrocnemius and hamstring muscles) from PAI-inhibitor treated than from vehicle-treated mice (Figure 1K-N). These data demonstrate that PAI inhibition accelerates ischemic tissue recovery.

Endogenous tPA and MMP-9 are required for the tissue-regenerative effects observed after PAI inhibition

We reported previously that the fibrinolytic factor tPA promotes angiogenesis and tissue regeneration in HL-ischemic tissue, which

Figure 1. PAI-1 inhibition improves HL-ischemic tissue regeneration. (A-E) C57BL/6 mice were HL treated and gastrocnemius muscles were analyzed on day 1. (A-C) Quantitative RT-PCR analysis of the mRNA expression of *PAI-1* (A), *uPA* (B), and *tPA* (C) in nonischemic and HL-ischemic muscle tissue using β-actin as an internal control (n = 3/group for all experiments). (D-E) Homogenates of ischemic and nonischemic tissues that were harvested on day 1 after HL-ischemia induction in 3 different C57BL/6 mice were assayed for murine PAI-1 protein by Western blot analysis (D) or for PAI activity by reverse fibrin zymography (E). Densitometric analysis is shown (bottom). (F-N) HL ischemia was induced in C57BL/6 mice, followed by oral administration of the PAI-1 inhibitor or vehicle given daily from days 0-6. Arrows indicate when the PAI inhibitor was administered. Plasma levels of active PAI-1 (F), tPA (G), and plasmin (H) were assayed in PAI-1- or vehicle-treated HL-ischemic mice by ELISA (n = 7/ group for PAI-1 and tPA; n = 6/group for plasmin). (I-J) Representative macroscopic images (I) and the limb perfusion ratio (ischemic/nonischemic; J) of ischemic limbs after HL-ischemia induction. Macroscopic evaluation of the limbs on day 21 (I, bottom) shows foot-digit necrosis only in HL + vehicle-treated animals (n = 5/group). (K-N) Muscle sections of a nonischemic limb and of gastrocnemius (K-L) and hamstring muscles (M-N) of the ischemic limbs from treated mice were stained with H&E (after 21 days; scale bars, 200 mm; K,M) and necrotic areas were evaluated (n = 4 for vehicle group; n = 3 for PAI-1 inhibitor group; L,N). Data represent means ± SEM. *P < .05; **P < .001.
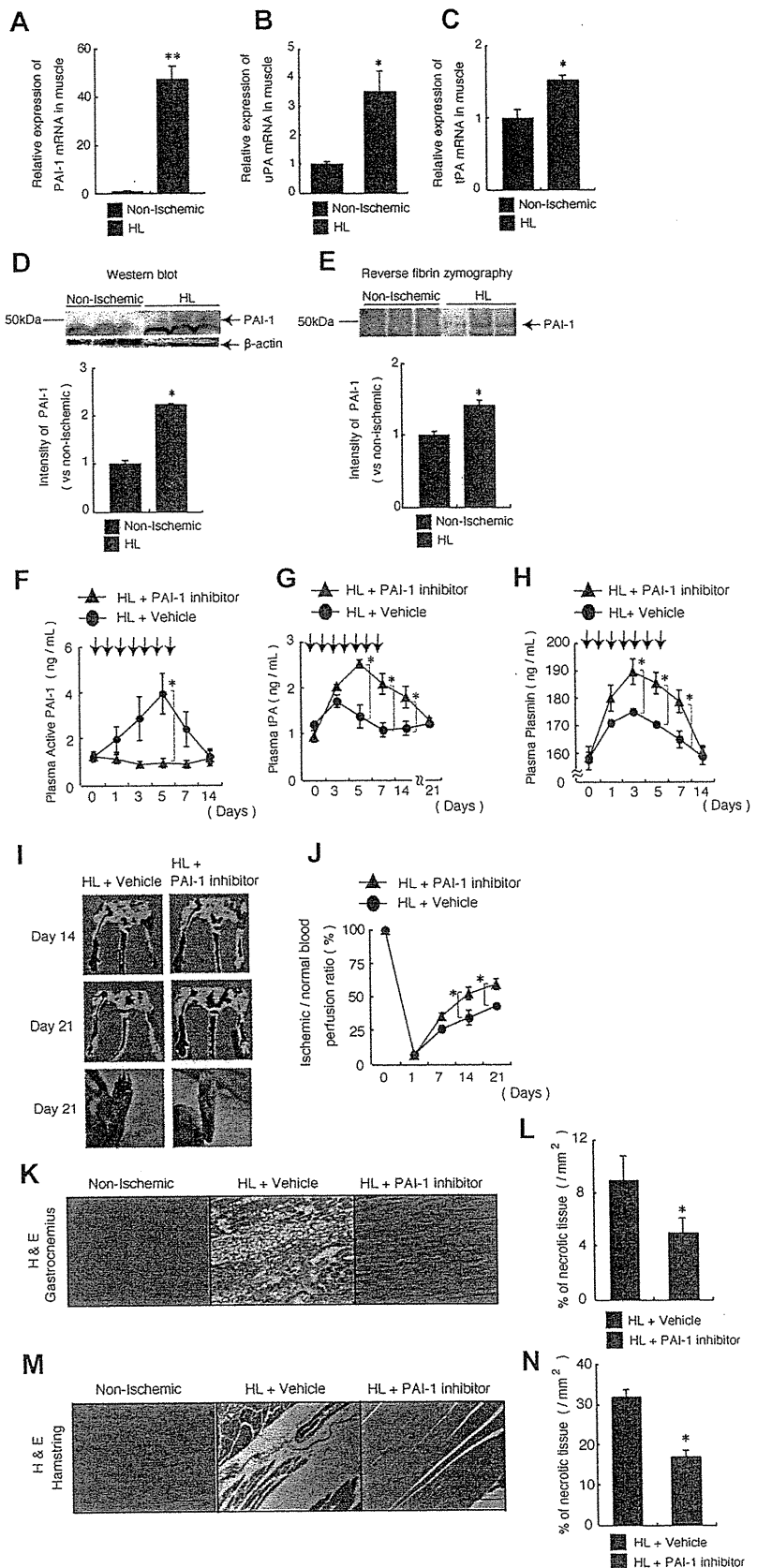
requires the up-regulation of MMP-9.[19] In the present study, we found that PAI-1 inhibitor treatment during ischemic recovery augmented fibrinolytic activity in blood samples from tPA^{+/+} mice, but not from tPA^{-/-} mice (Figure 2A), and augmented MMP-9

plasma levels during HL-ischemic recovery in tPA^{+/+} mice compared with vehicle-treated tPA^{+/+} mice, suggesting that increased tPA and MMP-9 may mediate the observed effects of PAI-I (Figure 2B). No change in MMP-9 plasma levels was observed in
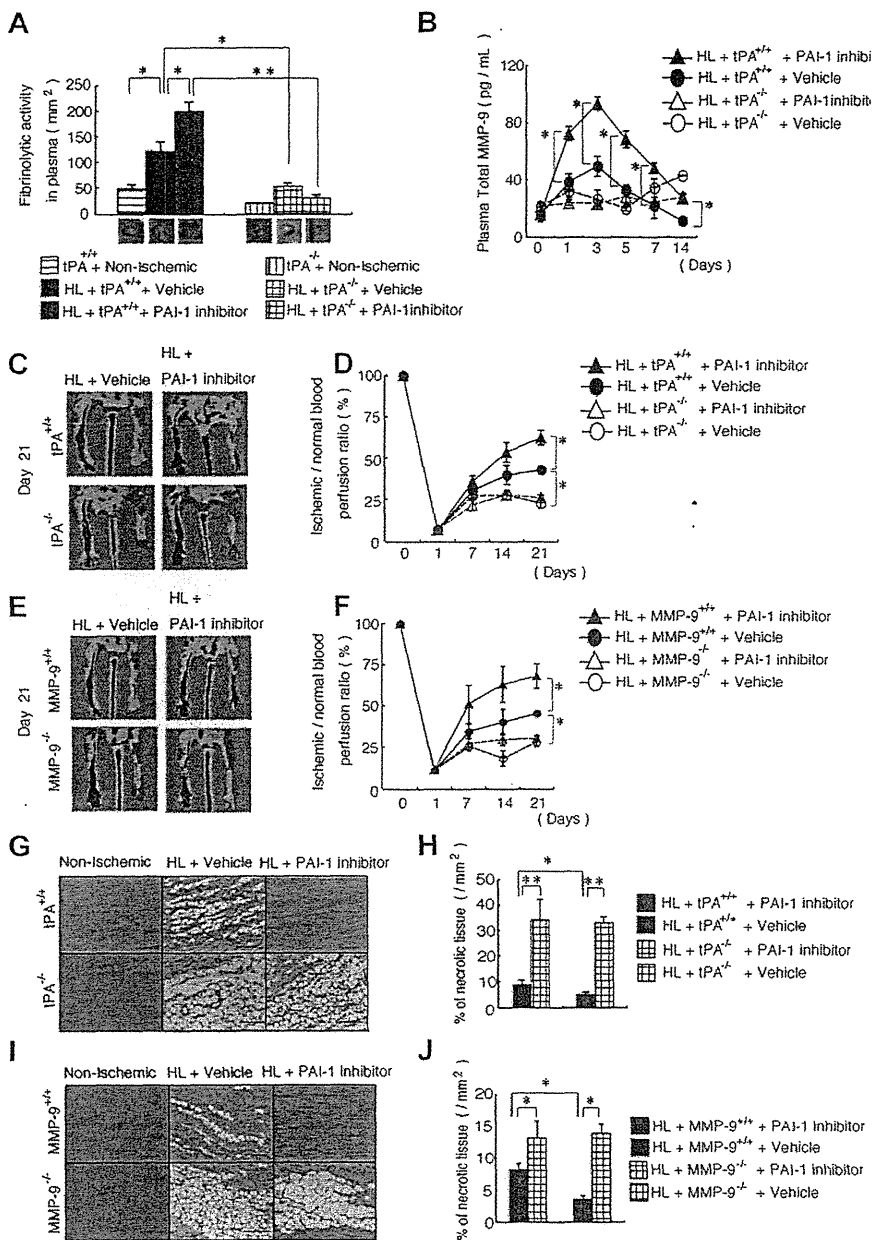
Figure 2. Improved ischemic tissue regeneration after PAI-1 inhibitor treatment depends on tPA and MMP-9. (A-J) HL ischemia was induced in tPA$^{+/+}$, tPA$^{-/-}$, MMP-9$^{+/+}$, and MMP-9$^{-/-}$ mice and the mice were then treated with or without PAI-1 inhibitor daily from days 0-6. (A) Fibrinolytic activity in plasma samples of HL-ischemia-induced tPA$^{+/+}$ and tPA$^{-/-}$ mice was analyzed on day 1 using a fibrin plate assay (n = 3/group). (B) MMP-9 plasma levels were determined in tPA$^{+/+}$ and tPA$^{-/-}$ mice treated with the PAI-1 inhibitor or with vehicle by ELISA (n = 9 for tPA$^{+/+}$ mice; n = 3 for tPA$^{-/-}$ mice). (C,E) Representative images of limb perfusion analyzed using a laser Doppler. (D,F) The limb perfusion ratio (ischemic/nonischemic) over time of tPA$^{+/+}$ and tPA$^{-/-}$ mice (D) and MMP-9$^{+/+}$ and MMP-9$^{-/-}$ mice (F) treated with the PAI-1 inhibitor or with vehicle (n = 3/group). (G-J) Necrotic areas in sections of H&E-stained muscle sections (G,I) from untreated and PAI-1 inhibitor-treated ischemic limbs (scale bars, 200 mm). (H,J) Necrotic areas in ischemic muscle tissue sections were evaluated after 21 days (n = 3/group). Data represent means ± SEM. *$P < .05$; **$P < .01$.

HL-ischemia–induced tPA$^{-/-}$ mice treated with vehicle or with the PAI-1 inhibitor (Figure 2B).

We next determined whether endogenous tPA and MMP-9 mediate the improved tissue regeneration that is observed after PAI-1 inhibitor treatment. Indeed, PAI-1 inhibitor treatment resulted in faster blood flow recovery in the ischemic limbs of wild-type mice compared with vehicle-treated wild-type mice, but such enhancement was not observed in tPA$^{-/-}$ mice or MMP-9$^{-/-}$ mice (Figure 2C-F). Ischemic tissue sections from PAI-1 inhibitor-treated tPA$^{-/-}$ and MMP-9$^{-/-}$ mice showed vast areas of necrotic tissue compared with PAI-1 inhibitor-treated tPA$^{+/+}$ and MMP-9$^{+/+}$ mice (Figure 2G-J). These data indicate that endogenous tPA and MMP-9 are required for the tissue-regeneration-promoting effects of PAI-1 inhibition.

PAI-1 inhibition improves tPA-dependent ischemic revascularization

PAI-1 inhibitor treatment resulted in faster collateral vessel growth, which was observed macroscopically (Figure 3A) and

microscopically after VWF staining in the ischemic limb of C57BL/6 mice (Figure 3B) and in the ischemic limb of tPA$^{+/+}$ mice compared with vehicle-treated mice (Figure 3C-D), but did not show such enhancement in the ischemic limb of tPA$^{-/-}$ mice. We have shown previously that tPA treatment increases VEGF-A plasma levels and that tPA administration can promote myeloid-cell expansion by MMP-9–mediated release of KitL from stromal/niche cells.[19] Indeed, augmented plasma levels of VEGF-A (Figure 3E) and KitL (Figure 3F) were found in PAI-1 inhibitor-treated HL-ischemic tPA$^{+/+}$ mice, but not in PAI-1 inhibitor-treated tPA$^{-/-}$ mice. Furthermore, G-CSF, a cytokine known to stimulate BM granulopoiesis, was also increased after PAI-1 inhibitor treatment in HL-ischemic mice in a MMP-9– and tPA-dependent manner (Figure 3G-H). In addition, recombinant tPA administration augmented G-CSF serum levels in normoxic C57BL/6 mice (Figure 3I). These data indicate that PAI-1 inhibition during ischemic recovery augments both angiogenic and hematopoietic factors.

Figure 3. In vivo blockade of PAI-1 augments neoangiogenesis and growth factor release. (A) Macroscopic images of the lower limb region of nonischemic and PAI-1 inhibitor- or vehicle-treated wild-type mice were captured on day 14 after HL ischemia induction (magnification, 25×; scale bars, 2000 mm). The insert box depicts areas of neoangiogenesis. (B-G) HL ischemia was induced in C57BL/6, tPA$^{+/+}$, and tPA$^{-/-}$ mice, and the mice were then treated with or without PAI-1 inhibitor daily from days 0-6. (B-C) Capillary density was measured in sections of the hamstring (B) and adductor muscles (C) based on immunohistochemical staining of VWF per high power field (HPF). (B,D) Representative images of anti-VWF mAb immunohistochemical staining of ischemic muscle sections from HL-ischemia–induced C57BL/6, tPA$^{+/+}$, and tPA$^{-/-}$ mice either left untreated or treated with or without the PAI-1 inhibitor (n = 6/group) analyzed on day 14 after the procedure (scale bars, 200 mm). Arrows depict VWF$^+$ capillaries. (E-G) Plasma levels of VEGF-A (E) and KitL (F) and serum levels of G-CSF (G) in HL-ischemia–induced tPA$^{+/+}$ and tPA$^{-/-}$ mice treated with or without PAI-1 inhibitor were determined by ELISA (for VEGF-A, n = 9 for tPA$^{+/+}$ mice and n = 3 for tPA$^{-/-}$ mice; for KitL and G-CSF, n = 7 for tPA$^{+/+}$ mice and n = 3 for tPA$^{-/-}$ mice; for KitL, n = 3 for G-CSF). (H) G-CSF serum levels were analyzed by ELISA in HL-ischemia–induced MMP-9$^{+/+}$ and MMP-9$^{-/-}$ mice treated with or without PAI-1 inhibitor (H) and in C57BL/6 mice treated with a serpin-resistant tPA mutant (n = 4-5/group). Values represent the means ± SEM. *P < .05; **P < .001.
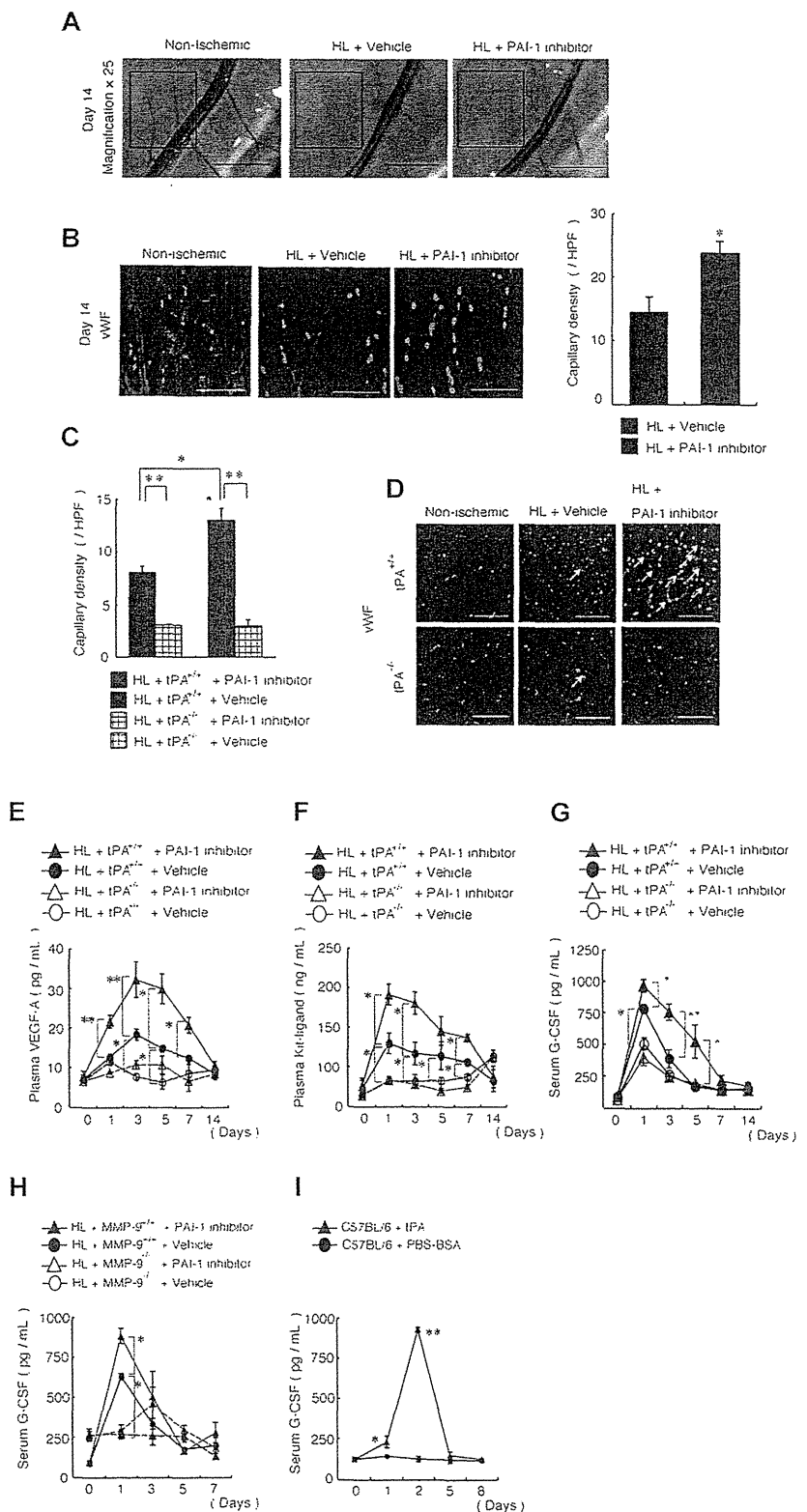
PAI-1 inhibition mobilizes neutrophils into the circulation and promotes neutrophil recruitment into ischemic tissues in vivo

The PAI-1 inhibitor-mediated increase in hematopoietic cytokines prompted us to examine whether the inflammatory response during ischemic recovery might be altered after PAI-1 inhibition. Isolation of leukocytes from ischemic muscle tissues, followed by MACS separation using the anti–Gr-1 Ab, revealed that approximately 40% of infiltrating leukocytes were neutrophils on day 5 of HL ischemia (Figure 4A). PAI-1 inhibitor treatment increased the number of Gr-1$^+$ neutrophils in ischemic sections of tPA$^{+/+}$ mice, but not in tPA$^{-/-}$ mice, compared with vehicle-treated mice (Figure 4B-C).
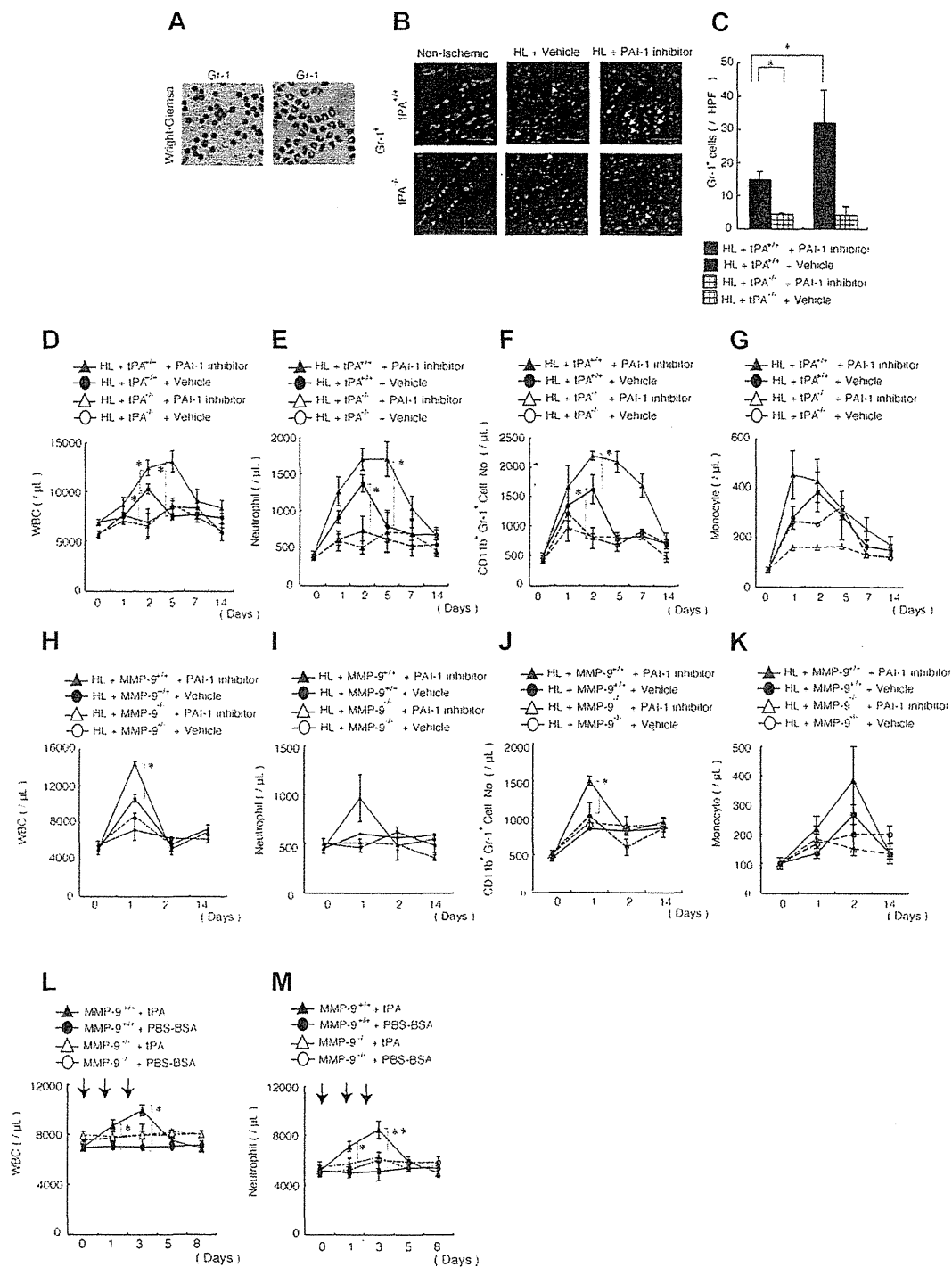
Figure 4. Pharmacologic PAI inhibition mobilizes neutrophils into the circulation and improves their tissue infiltration, a process dependent on endogenous tPA and MMP-9. (A) Wright-Giemsa staining of MACS-isolated infiltrating Gr-1+ and Gr-1− cells derived from ischemic tissues of C57BL/6 mice on day 5 after HL induction. (B) Immunofluorescent staining of Gr-1 was performed on nonischemic muscle tissues or on HL-ischemic muscle tissues derived from vehicle- or PAI-1 inhibitor-treated HL-ischemic tPA+/+ and tPA−/− mice 14 days after the HL procedure. PAI-1 inhibitor was administered daily on days 0-6 after the procedure. The arrows indicate Gr-1+ cells (scale bars, 200 mm). Nuclei were counterstained with DAPI (blue). (C) Quantification of Gr-1+ cells in ischemic muscle tissues (n = 3/group). (D-K) The total number of WBCs (D,H) and the number of neutrophils (E,I), CD11b+Gr-1+ cells (F,J), and monocytes (G,K) were determined in the peripheral blood of PAI-1 inhibitor-treated or vehicle-treated tPA+/+ and tPA−/− mice (for B-G, n = 4) and in MMP-9+/+ and MMP-9−/− mice (for H-K, n = 6) by counting (D,E,G,H,I,K) or by FACS analysis (F,J). (L-M) The total number of WBCs (L) and neutrophils (M) were counted in in MMP-9+/+ and MMP-9−/− mice (n = 4). *P < .05; **P < .001 for recombinant tPA-treated versus vehicle-treated C57BL/6 mice. Values represent the means ± SEM. Data are expressed as the absolute number of each cell type per milliliter of blood. *P < .05.

We next analyzed blood samples to determine whether the augmented neutrophil influx in ischemic tissues was due to an overall increase in circulating blood cells. PAI-1 inhibitor-treated HL-ischemic tPA+/+ mice, but not tPA−/− mice, showed an increase in the number of WBCs, including neutrophils, as determined by cell counting and FACS analysis using Abs against CD11b and Gr-1 (Figure 4D-F), but not monocytes, compared with vehicle-treated animals (Figure 4G). MMP-9 deficiency prevented the leukocyte and neutrophil increase, but not the monocyte increase, caused by PAI-1 inhibitor treatment (Figure 4H-K), indicating that PAI-1 inhibitor-mediated neutrophilia was dependent on endogenous MMP-9. Administration of recombinant tPA

Figure 5. Adoptive transfer of Gr-1⁺ cells from PAI-1 inhibitor-treated mice improves neoangiogenesis. (A-F) Muscle-derived Gr-1⁺ cells isolated from HL-ischemia–induced-C57BL/6 donors treated with/without PAI-1 inhibitor were transplanted into HL-ischemia–induced recipients for 3 days (n = 6/group). (A) Experimental scheme of the muscle-derived Gr-1⁺ cell transplantation assay. (B) Blood flow was determined after transplantation of PAI-1 inhibitor-mobilized versus vehicle-mobilized (mob.) Gr-1⁺ cells in HL-ischemic C57BL/6 recipients. (C) VWF immunostaining of lower limb ischemic tissue of mice receiving vehicle- or PAI-1 inhibitor-mobilized cell transplantations. Arrows indicate capillaries. Nuclei were counterstained with DAPI (blue staining). Scale bars indicate 200 mm. (D) Capillary density was evaluated per high-power field (HPF). (E) Immunofluorescent staining of Gr-1 and VEGF-A was performed on sections derived from vehicle or PAI-1 inhibitor-mobilized Gr-1 cell-transplanted mice. The arrows indicate transplanted Gr-1⁺ cells costained with VEGF-A in ischemic tissues. Nuclei were counterstained with DAPI (blue). (F) Quantification of Gr-1⁺ VEGF-1⁺ cells under a HPF. Data represent means ± SEM. *P < .05.
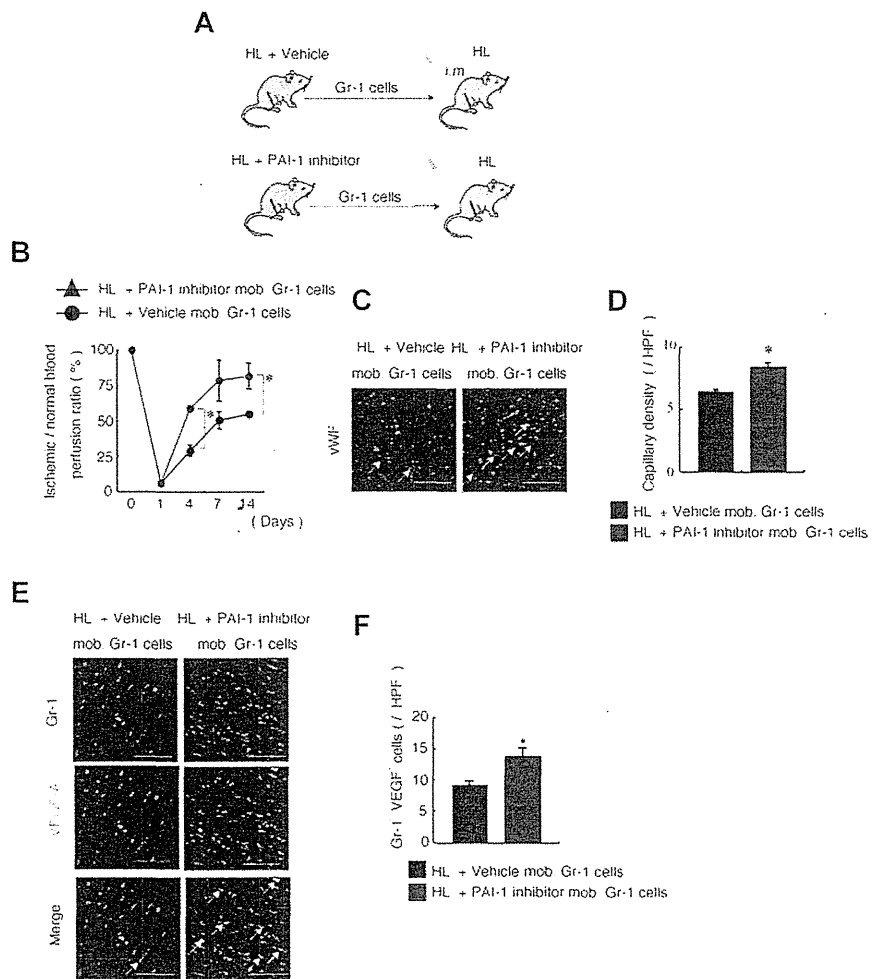
induced neutrophilia and, similar to PAI-1 inhibitor administration, this process required endogenous MMP-9 (Figure 4L-M). Therefore, PAI-1 inhibitor treatment not only augmented the absolute number of circulating Gr-1⁺ cells/neutrophils, but also improved their incorporation into ischemic tissues in a tPA- and MMP-9–dependent manner.

Adoptive transfer of Gr-1⁺ myeloid cells from PAI-1 inhibitor-treated mice improves revascularization after HL ischemia induction

Our data suggested that neutrophils could be the cellular target for PAI-1 inhibitor-induced improved tissue regeneration. We hypothesized that PAI-1 induction during HL ischemia may alter the ability of neutrophils to stimulate angiogenesis. To test this hypothesis, muscle-derived Gr-1⁺ cells were obtained from HL-ischemia–induced donor mice that had been treated with or without the PAI-1 inhibitor. These Gr-1⁺ cells were transplanted into HL recipient mice (Figure 5A) by intramuscular injection. In contrast to cells from vehicle-treated mice, Gr-1⁺ cells isolated from muscle tissues of PAI-1 inhibitor-treated mice accelerated ischemic reperfusion (Figure 5B) and increased capillary density in ischemic tissues of HL-ischemic recipients (Figure 5C-D). We showed that neutrophils release the proangiogenic factor VEGF-A.[21] Consistent with that result, the absolute number of Gr-1⁺VEGF-1⁺ cells was higher in ischemic recipient tissues transplanted with Gr-1⁺ cells from PAI-1–treated mice (Figure 5E-F).

These data indicate that PAI-1 inhibitor-mediated neoangiogenesis is partially driven by a Gr-1⁺ muscle-residing cell population.

The proangiogenic PAI-1 inhibitor enhances FGF-2 and VEGF-A function/signaling

We reported previously that a serpin-resistant tPA promoted macrophage-mediated angiogenesis.[22] To determine whether PAI-1 inhibition accelerates macrophage recruitment into ischemic tissues, we quantified the number of infiltrating F4/80⁺ cells 3 days after initiation of HL ischemia. PAI-1 inhibition did not increase the recruitment of macrophages in muscle tissues compared with vehicle treatment (Figure 6A).

To identify the molecular mechanisms underlying the enhanced angiogenesis observed after PAI-1 inhibition, we examined the expression of angiogenesis-related factors in ischemic muscle tissues derived from PAI-1 inhibitor- and vehicle-treated animals. FGF-2 signaling has been associated with neutrophil-mediated angiogenesis[23] and PAI-1 activity.[22] Immunohistochemical analysis of ischemic muscle tissues demonstrated that the number of F4/80⁺ cells coexpressing FGF-2 or VEGF-A was not significantly different from vehicle- and PAI-1 inhibitor-treated tissues (Figure 6B). In contrast, the number of ischemic tissue-resident Gr-1⁺ cells coexpressing both FGF-2 and VEGF-A was higher in sections derived from PAI-1 inhibitor-treated mice (Figure 6C).

FGF-2 can signal through syndecan-4 independently of FGF receptors.[22] Therefore, in the present study, we investigated whether
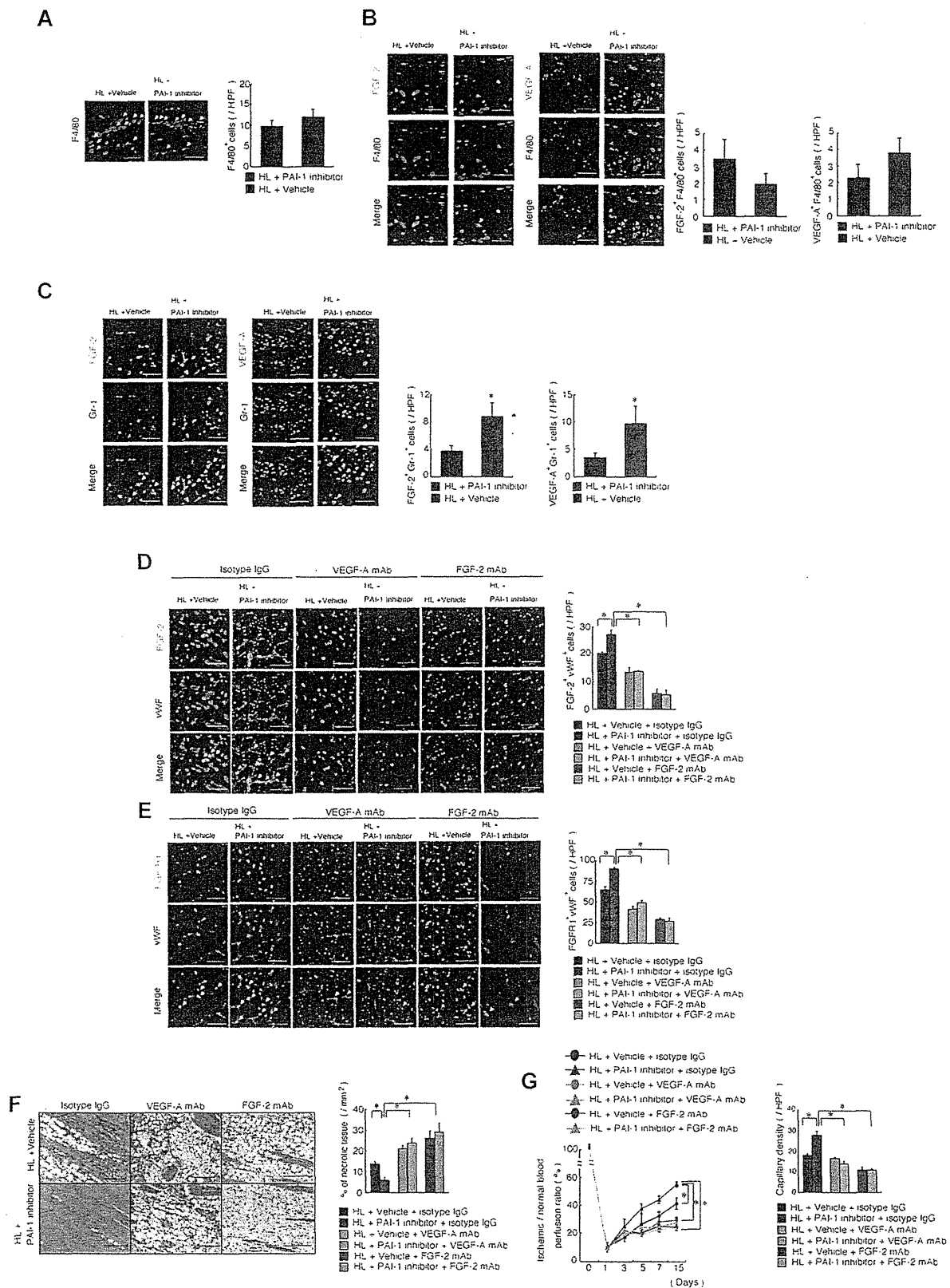
Figure 6. PAI-inhibition induces angiogenesis during HL-ischemic recovery via FGF-2- and VEGF-A–mediated pathways. (A-C) HL-ischemia–induced C57BL/6 mice were treated with the PAI-1 inhibitor or vehicle. Ischemic sections of PAI-1 inhibitor or vehicle-treated mice 3 days after the HL procedure were costained for F4/80 (A), F4/80 and VEGF-A or F4/80 and FGF-2 (B), or Gr-1 and VEGF-A or Gr-1 and FGF-2 (C). Nuclei were counterstained with DAPI (blue). Left panels are representative immunofluorescent images. Arrows indicate VEGF-A+, FGF-2+, F4/80+, or Gr-1+ cells. Right panel shows the quantification of the indicated cell populations per high-power field (HPF; n = 5/group for each experiment). (D-G) HL-ischemia–induced C57BL/6 mice were treated with the PAI-1 inhibitor and coinjected with neutralizing doses of anti–FGF-2, anti–VEGF-A, or anti–IgG control Abs (n = 4/group). (D-E) Ischemic muscle tissues from Ab-treated animals 14 days after the HL procedure were immunofluorescently costained for FGF-2/VWF and FGF-R1/VWF. Nuclei were counterstained with DAPI (blue staining). Arrows indicate FGF-2+/VWF+ and FGF-R1+/VWF+ cells (scale bars, 200 mm). Right panel shows the indicated cell populations quantified per HPF. (F) Left panel, ischemic muscle tissue sections were stained with H&E (scale bars, 200 mm). Right panel shows the quantification of necrotic areas in ischemic H&E-stained tissue sections. (G) Blood flow was determined at the indicated time points. (H) Ischemic muscle tissue sections stained with Abs against VWF antigen on day 14 were used to determine capillary density. Data represent means ± SEM. *P < .05.

Figure 7. Schematic diagram showing the various molecules involved in the proangiogenic effect of PAI-1 inhibition. Under ischemic conditions, the local balance between the fibrinolytic factor tPA and one of its endogenous inhibitors, PAI-1, is shifted toward a profibrinolytic state with a local increase in tPA. Ischemia systemically results in a profibrinolytic state, a process dependent on endogenous tPA. Pharmacologic PAI-1 inhibition during ischemic recovery improved tissue regeneration due to an expansion of circulating and tissue-resident Gr-1+ neutrophils coexpressing VEGF-A, FGF-2, and TIMP-1–free MMP-9, and to increased release of the angiogenic factor VEGF-A, the hematopoietic growth factor KitL, and G-CSF. Ab neutralization and genetic-knockout studies indicated that both the improved tissue regeneration and the increase in both circulating and ischemic tissue-resident Gr-1+ neutrophils were dependent on the activation of tPA and MMP-9 and on VEGF-A and FGF-2.
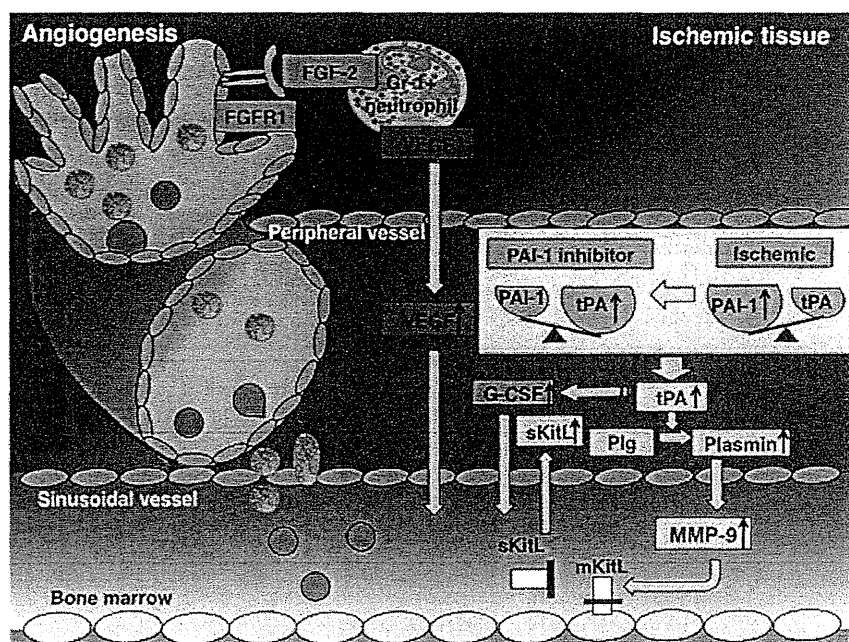
expression of FGF-2 or FGFR1 is altered in PAI-1 inhibitor-treated ischemic tissues. Immunohistochemical analysis of ischemic muscle tissue sections revealed that PAI-1 inhibitor treatment augmented FGF-2 and FGF-R1 expression and that this expression colocalized more often to VWF+ cells compared with vehicle-treated controls (Figure 6D-E).

FGF-2–induced angiogenesis requires VEGF signaling.[24] Blockade of VEGF-A and FGF-2 signaling with Abs against murine VEGF-A and FGF-2 inhibited the PAI-1 inhibitor-mediated FGF-2 and FGFR-1 increase on VWF+ cells (Figure 6D-E), as well as the PAI-1 inhibitor-mediated ischemic tissue recovery, and reversed the necrosis-reducing effect of PAI-1 inhibitor treatment (Figure 6F-G) and myeloid cell mobilization (supplemental Figure 1A-C, available on the *Blood* Web site; see the Supplemental Materials link at the top of the online article) in an HL-ischemic model.

Although it is clear that FGF-2–induced angiogenesis requires VEGF signaling,[24] it was unclear whether VEGF-A and FGF-2 signaling are required for PAI-1 inhibitor-mediated tissue neoangiogenesis. Our present data suggest that this might be the case, because VEGF-A and FGF-2 mAb prevented PAI-1 inhibitor-mediated ischemic tissue recovery and neoangiogenesis in an HL-ischemic model (Figure 6F-G).

The results of the present study indicate that the proangiogenic effects observed after PAI-1 inhibitor treatment are mediated by the 2 potent proangiogeneic factors FGF-2 and VEGF-A, and that neutrophils seem to be a source for these growth factors. In addition, both factors were essential for the PAI-1 inhibitor-mediated recruitment of "angiogenic hematopoietic effector cells" into ischemic tissues.

Discussion

The present study identifies activation of the FGF-2 and VEGF-A pathways as the cause of the proangiogeneic effect of drug-induced PAI-1 deficiency in a murine model of HL ischemia. Our data support a mechanism whereby drug-induced PAI-1 inhibition enhances angiogenesis through up-regulation of endogenous tPA

and MMP-9. Both proteases are required for neutrophil mobilization and for the release of proangiogenic cytokines, including FGF-2 and VEGF-A (Figure 7). In addition, muscle-infiltrating CD11b+Gr-1+ neutrophils harvested from PAI-1 inhibitor-treated mice coexpressed FGF-2 and VEGF-A and showed an improved capacity to stimulate angiogenesis on adoptive transfer compared with equal numbers of carrier-treated ischemic tissue-derived neutrophils. Ab-blocking experiments revealed that PAI-inhibitor–induced tissue regeneration required FGF-2 and VEGF-A signaling. These data are important for the design of future cell-based therapies, especially in the light of a recent study demonstrating that BM cells harvested from mice with distant ischemia show a reduced capacity to stimulate angiogenesis on adoptive transfer.[25]

FGF family members and its receptors (FGFRs) can promote angiogenesis. In the present study, PAI-1 inhibition-induced augmentation of FGFR1 expression on endothelial cells in ischemic tissues coincided with increased KitL plasma levels. This result is consistent with a previous study showing that FGFR-1–deficient embryoid bodies show decreased expression of KitL.[26] KitL can improve tissue recovery in animal models of HL ischemia.[27-29] Recombinant tPA therapy augments circulating KitL levels[30] and promotes ischemic revascularization.[19] Confirming these data, in the present study, we found that drug-induced PAI-1 inhibition raised KitL plasma levels via tPA augmentation. Our data imply a relationship among the fibrinolytic factors PAI-1/tPA, FGFR1 signaling, and KitL production. However, further studies are required to determine how these pathways interact with each other.

PAI-1 in cooperation with integrins, coagulation, fibrinolysis, and endocytosis has been shown to be important for macrophage migration.[7] In the present study, we show that pharmacologic blockade of PAI-1 increased MMP-9– and tPA-dependent augmentation of tissue-residing neutrophils, but not F4/80+ macrophages, under ischemic conditions. Therefore, PAI-1 seems to act as a negative regulator of neutrophil recruitment during HL-ischemic recovery. Supporting our observations, Renckens et al demonstrated that PAI-1 gene-deficient mice showed an enhanced early influx of neutrophils to the site of inflammation in a murine model of turpentine-induced tissue injury.[31] In this model, no difference

was found between PAI-1$^{-/-}$ and PAI-1$^{+/+}$ mice in factors known to attract neutrophils, including keratinocyte-derived chemokine and macrophage inflammatory protein-2.

Among the factors that can enhance the survival, proliferation, differentiation, and function of neutrophil precursors and mature neutrophils[32] is the hematopoietic growth factor G-CSF. In the present study, we demonstrate for the first time that recombinant tPA and endogenous tPA that is enhanced by PAI-1 inhibition promote the release of G-CSF. G-CSF has been shown to improve tissue recovery in animal models of HL[21] and myocardial[33] and focal cerebral ischemia injuries in both mice and humans[34] by modulating various cell types, including endothelial cells and neutrophils.[21,32] Various studies have demonstrated the importance of MMP-9 for neutrophil-driven neoangiogenesis in an HL-ischemic model.[2,19,21,35] A recent study demonstrated that tissue-infiltrating neutrophil pro-MMP-9 induces angiogenesis catalytically via an FGF-2/FGFR2 pathway.[23] Consistent with that study, we have shown previously that pharmacologic PAI-1 inhibition results in the accumulation of FGF-2– and VEGF-A–expressing Gr-1$^+$ neutrophils within ischemic muscle tissues through an effect on endogenous tPA and MMP-9, and in an increase of plasma VEGF-A via up-regulation of endogenous tPA.[19] Neutrophils can secrete tissue inhibitors of metalloproteinase (TIMP)–free MMP-9 that can act in concert with, for example, macrophages to liberate proangiogenic growth factors such as VEGF and FGF-2 that are sequestered to the extracellular matrix.

PAI-1 can inhibit cell adhesion and migration by inhibiting the activity of uPA receptor (uPAR)–bound uPA and by preventing integrin association to vitronectin. Studies with uPAR$^{-/-}$ mice have emphasized the critical role of this receptor in leukocyte trafficking.[31] Indeed, uPAR$^{-/-}$ mice displayed a profoundly reduced neutrophil recruitment to the peritoneal cavity after IP administration of thioglycollate.[36] Our present results are consistent with the findings that neutrophil extravasation into the interstitium after lung ischemia-reperfusion injury after lung transplantation was blocked in tPA-deficient mice.[37] At the molecular level, this blockage was associated with reduced expression of platelet endothelial cell adhesion molecule-1 mediated through the tPA/low-density lipoprotein receptor–related protein/NF-κB signaling pathway.

Reichel et al showed that extravasated plasmin(ogen) mediates neutrophil recruitment in vivo via activation of perivascular mast cells and secondary generation of lipid mediators.[38]

The combined data suggest that strategies aimed at inactivation of PAI-1 (eg, the use of the small-molecule TM5275) could be an immediately clinically applicable therapeutic option for improving angiogenesis in ischemic patients. The results of the present study shed new light on the mechanism by which PAI-1 and tPA enhance neovascularization by modulation of the local and systemic growth factor environment and by alteration of neutrophil migration.

Authorship

Contribution: Y.T., C.N., and K.S.-K. designed and performed the experiments, analyzed the data, and wrote the manuscript; M.O.-K. and M.I. designed and performed the experiments; A.S., I.G., H.K., and Y.S. developed the analytical tools; T.D., T.M., and Y.T. provided reagents; K.O., K.S., and H.N. provided technical support and conceptual advice; and B.H. and K.H. designed the experiments, analyzed the data, and wrote the manuscript.

Conflict-of-interest disclosure: The authors declare no competing financial interests.

Correspondence: Koichi Hattori, Center for Stem Cell Biology and Regenerative Medicine, Institute of Medical Science, University of Tokyo, 4-6-1, Shirokanedai, Minato-ku, Tokyo 108-8639, Japan; e-mail: khattori@ims.u-tokyo.ac.jp.

References

1. Carmeliet P. Mechanisms of angiogenesis and arteriogenesis. Nat Med. 2000;6(4):389.

2. Heissig B, Nishida C, Tashiro Y, et al. Role of neutrophil-derived matrix metalloproteinase-9 in tissue regeneration. Histol Histopathol. 2010; 25(6):765-770.

3. Simons M, Ware JA. Therapeutic angiogenesis in cardiovascular disease. Nat Rev Drug Discov. 2003;2(11):863-871.

4. Heissig B, Hattori K, Friedrich M, Rafii S, Werb Z. Angiogenesis: vascular remodeling of the extracellular matrix involves metalloproteinases. Curr Opin Hematol. 2003;10(2):136-141.

5. Dellas C, Loskutoff DJ. Historical analysis of PAI-1 from its discovery to its potential role in cell motility and disease. Thromb Haemost. 2005; 93(4):631-640.

6. Stefansson S, Lawrence DA. The serpin PAI-1 inhibits cell migration by blocking integrin alpha V beta 3 binding to vitronectin. Nature. 1996; 383(6599):441-443.

7. Cao C, Lawrence DA, Li Y, et al. Endocytic receptor LRP together with tPA and PAI-1 coordinates Mac-1-dependent macrophage migration. EMBO J. 2006;25(9):1860-1870.

8. Carmeliet P, Moons L, Lijnen R, et al. Inhibitory role of plasminogen activator inhibitor-1 in arterial wound healing and neointima formation: a gene targeting and gene transfer study in mice. Circulation. 1997;96(9):3180-3191.

9. Fay WP, Shapiro AD, Shih JL, Schleef RR, Ginsburg D. Brief report: complete deficiency of plasminogen-activator inhibitor type 1 due to a frame-shift mutation. N Engl J Med. 1992; 327(24):1729-1733.

10. Sawdey MS, Loskutoff DJ. Regulation of murine type 1 plasminogen activator inhibitor gene expression in vivo. Tissue specificity and induction by lipopolysaccharide, tumor necrosis factor-alpha, and transforming growth factor-beta. J Clin Invest. 1991;88(4):1346-1353.

11. Sakamoto T, Yasue H, Ogawa H, Misumi I, Masuda T. Association of patency of the infarct-

related coronary artery with plasma levels of plasminogen activator inhibitor activity in acute myocardial infarction. Am J Cardiol. 1992;70(3):271-276.

12. Juhan-Vague I, Pyke SD, Alessi MC, Jespersen J, Haverkate F, Thompson SG. Fibrinolytic factors and the risk of myocardial infarction or sudden death in patients with angina pectoris. ECAT Study Group. European Concerted Action on Thrombosis and Disabilities. Circulation. 1996;94(9):2057-2063.

13. Diebold I, Kraicun D, Bonello S, Gorlach A. The 'PAI-1 paradox' in vascular remodeling. Thromb Haemost. 2008;100(6):984-991.

14. Stefansson S, McMahon GA, Petitclerc E, Lawrence DA. Plasminogen activator inhibitor-1 in tumor growth, angiogenesis and vascular remodeling. Curr Pharm Des. 2003;9(19):1545-1564.

15. McMahon GA, Petitclerc E, Stefansson S, et al. Plasminogen activator inhibitor-1 regulates tumor growth and angiogenesis. J Biol Chem. 2001; 276(36):33964-33968.

16. van Meijer M, Smilde A, Tans G, Nesheim ME, Pannekoek H, Horrevoets AJG. The suicide substrate reaction between plasminogen activator inhibitor 1 and thrombin is regulated by the cofactors vitronectin and heparin. *Blood.* 1997;90(5): 1874-1882.

17. Lijnen HR, Arza B, Van Hoef B, Collen Ds Declerck PJ. Inactivation of plasminogen activator inhibitor-1 by specific proteolysis with stromelysin-1 (MMP-3). *J Biol Chem.* 2000; 275(48):37645-37650.

18. Izuhara Y, Yamaoka N, Kodama H, et al. A novel inhibitor of plasminogen activator inhibitor-1 provides antithrombotic benefits devoid of bleeding effect in non-human primates. *J Cereb Blood Flow Metab.* 2010;30(5):904-912.

19. Ohki M, Ohki Y, Ishihara M, et al. Tissue type plasminogen activator regulates myeloid-cell dependent neoangiogenesis during tissue regeneration. *Blood.* 2010;115(21):4302-4312.

20. Loskutoff DJ, Sawdey M, Keeton M, Schneiderman J. Regulation of PAI-1 gene expression in vivo. *Thromb Haemost.* 1993;70(1): 135-137.

21. Ohki Y, Heissig B, Sato Y, et al. Granulocyte colony-stimulating factor promotes neovascularization by releasing vascular endothelial growth factor from neutrophils. *FASEB J.* 2005;19(14): 2005-2007.

22. Drinane M, Walsh J, Mollmark J, Simons M, Mulligan-Kehoe MJ. The anti-angiogenic activity of rPAI-1(23) inhibits fibroblast growth factor-2 functions. *J Biol Chem.* 2006;281(44):33336-33344.

23. Ardi VC, Van den Steen PE, Opdenakker G,

Schweighofer B, Deryugina EI, Quigley JP. Neutrophil MMP-9 proenzyme, unencumbered by TIMP-1, undergoes efficient activation in vivo and catalytically induces angiogenesis via a basic fibroblast growth factor (FGF-2)/FGFR-2 pathway. *J Biol Chem.* 2009;284(38):25854-25866.

24. Murakami M, Simons M. Fibroblast growth factor regulation of neovascularization. *Curr Opin Hematol.* 2008;15(3):215-220.

25. Gregory AD, Capoccia BJ, Woloszynek JR, Link DC. Systemic levels of G-CSF and interleukin-6 determine the angiogenic potential of bone marrow resident monocytes. *J Leukoc Biol.* 2010;88(1):123-131.

26. Magnusson PU, Dimberg A, Mellberg S, Lukinius A, Claesson-Welsh L. FGFR-1 regulates angiogenesis through cytokines interleukin-4 and pleiotrophin. *Blood.* 2007;110(13):4214-4222.

27. Jin DK, Shido K, Kopp HG, et al. Cytokine-mediated deployment of SDF-1 induces revascularization through recruitment of CXCR4+ hemangiocytes. *Nat Med.* 2006;12(5):557-567.

28. Heissig B, Werb Z, Rafii S, Hattori K. Role of c-kit/Kit ligand signaling in regulating vasculogenesis. *Thromb Haemost.* 2003;90(4):570-576.

29. Heissig B, Rafii S, Akiyama H, et al. Low-dose irradiation promotes tissue revascularization through VEGF release from mast cells and MMP-9-mediated progenitor cell mobilization. *J Exp Med.* 2005;202(6):739-750.

30. Heissig B, Lund LR, Akiyama H, et al. The plasminogen fibrinolytic pathway is required for hematopoietic regeneration. *Cell Stem Cell.* 2007; 1(6):658-670.

31. Renckens R, Roelofs JJTH, De Waard V, et al.

The role of plasminogen activator inhibitor type 1 in the inflammatory response to local tissue injury. *J Thromb Haemost.* 2005;3(5):1018-1025.

32. Park K-W, Kwon Y-W, Cho H-J, et al. G-CSF exerts dual effects on endothelial cells-Opposing actions of direct eNOS induction versus indirect CRP elevation. *J Mol Cell Cardiol.* 2008;45(5): 670-678.

33. Kanellakis P, Slater NJ, Du XJ, Bobik A, Curtis DJ. Granulocyte colony-stimulating factor and stem cell factor improve endogenous repair after myocardial infarction. *Cardiovasc Res.* 2006;70(1):117-125.

34. Minnerup J, Heidrich J, Wellmann J, Rogalewski A, Schneider A, Schabitz WR. Meta-analysis of the efficacy of granulocyte-colony stimulating factor in animal models of focal cerebral ischemia. *Stroke.* 2008; 39(6):1855-1861.

35. Muhs BE, Gagne P, Plitas G, Shaw JP, Shamamian P. Experimental hindlimb ischemia leads to neutrophil-mediated increases in gastrocnemius MMP-2 and -9 activity: a potential mechanism for ischemia induced MMP activation. *J Surg Res.* 2004;117(2):249-254.

36. May AE, Kanse SM, Lund LR, Gisler RH, Imhof BA, Preissner KT. Urokinase receptor (CD87) regulates leukocyte recruitment via beta 2 integrins in vivo. *J Exp Med.* 1998;188(6):1029-1037.

37. Zhao Y, Sharma AK, LaPar DJ, et al. Depletion of tissue plasminogen activator attenuates lung ischemia-reperfusion injury via inhibition of neutrophil extravasation. *Am J Physiol Lung Cell Mol Physiol.* 2011;300(5):L718-L729.

38. Reichel CA, Lerchenberger M, Uhl B, et al. Plasmin inhibitors prevent leukocyte accumulation and remodeling events in the postischemic microvasculature. *PLoS One.* 2011;6(2):e17229.

ORIGINAL ARTICLE

Plasmin inhibitor reduces T-cell lymphoid tumor growth by suppressing matrix metalloproteinase-9-dependent CD11b⁺/F4/80⁺ myeloid cell recruitment

M Ishihara[1], C Nishida[1], Y Tashiro[1], I Gritli[1], J Rosenkvist[1], M Koizumi[1], Y Okaji[2], R Yamamoto[3], H Yagita[4], K Okumura[5], M Nishikori[6], K Wanaka[7], Y Tsuda[8], Y Okada[8], H Nakauchi[3], B Heissig[1,2,5,9] and K Hattori[1,5,9]

[1]Laboratory of Stem Cell Regulation, Center for Stem Cell Biology and Regenerative Medicine, Institute of Medical Science, University of Tokyo, Tokyo, Japan; [2]Frontier Research Initiative, Institute of Medical Science, University of Tokyo, Tokyo, Japan; [3]Laboratory of Stem Cell Therapy, Center for Experimental Medicine, Institute of Medical Science, University of Tokyo, Tokyo, Japan; [4]Department of Immunology, Juntendo University School of Medicine, Tokyo, Japan; [5]Atopy (Allergy) Research Center, Juntendo University School of Medicine, Tokyo, Japan; [6]Department of Hematology and Oncology, Kyoto University, Kyoto, Japan; [7]Kobe Research Projects on Thrombosis and Haemostasis, Kobe, Japan and [8]Faculty of Pharmaceutical Sciences, Kobe Gakuin University, Kobe, Japan

Activation of the fibrinolytic system during lymphoma progression is a well-documented clinical phenomenon. But the mechanism by which the fibrinolytic system can modulate lymphoma progression has been elusive. The main fibrinolytic enzyme, plasminogen (Plg)/plasmin (Plm), can activate matrix metalloproteinases (MMPs), such as MMP-9, which has been linked to various malignancies. Here we provide the evidence that blockade of Plg reduces T-cell lymphoma growth by inhibiting MMP-9-dependent recruitment of CD11b⁺F4/80⁺ myeloid cells locally within the lymphoma tissue. Genetic Plg deficiency and drug-mediated Plm blockade delayed T-cell lymphoma growth and diminished MMP-9-dependent CD11b⁺F4/80⁺ myeloid cell infiltration into lymphoma tissues. A neutralizing antibody against CD11b inhibited T-cell lymphoma growth in vivo, which indicates that CD11b⁺ myeloid cells have a role in T-cell lymphoma growth. Plg deficiency in T-cell lymphoma-bearing mice resulted in reduced plasma levels of the growth factors vascular endothelial growth-A and Kit ligand, both of which are known to enhance myeloid cell proliferation. Collectively, the data presented in this study demonstrate a previously undescribed role of Plm in lymphoproliferative disorders and provide strong evidence that specific blockade of Plg represents a promising approach for the regulation of T-cell lymphoma growth.

Introduction

Lymphomas are a heterogeneous group of malignancies of the lymphoid system that account for ~75 000 new tumor cases every year. In lymphoma patients, activation of the fibrinolytic system is frequently reported.[1] However, the mechanism by which the fibrinolytic system modulates tumor/lymphoma growth is not well understood. The fibrinolytic system is known to dissolve fibrin blood clots (fibrinolysis).[2] The serine proteinase plasminogen (Plg) is the main component of the fibrinolytic system and can be converted to the active enzyme, plasmin (Plm), by distinct Plg activators (PA), such as tissue-type Plg activator and urokinase-type Plg activator, which leads to fibrinolysis. The activities of tissue-type Plg activator and urokinase-type Plg activator are regulated by complex formation with PA inhibitors. Aside from fibrinolysis, Plm can activate several matrix metalloproteinases (MMPs) in vitro[3] and in vivo,[4] which are linked to tissue remodeling and various diseases, including lymphoid malignancy. Increased plasma MMP-9 levels were reported in Hodgkin's and non-Hodgkin's lymphoma patients.[5] But the distinct role of MMP-9 and the relation between Plg and MMP-9 in lymphoma growth is still not clear.

The biological and clinical behavior of, for example, T-cell lymphomas, which ranges from aggressive to indolent clinical features, is determined by the balance between tumor growth-supporting and tumor growth-repressive factors in the non-malignant microenvironment together with contributions from hematopoietic cells.[6]

The tumor microenvironment can influence neoplastic progression and growth.[7] MMPs are secreted as inactive pro-forms and are involved in angiogenesis, cytokine processing, extracellular matrix degradation and invasion during tumor progression.[8,9] In spite of the importance of MMPs during lymphoma growth, attempts to use MMP inhibitors in cancer therapy have been disappointing in clinical trials due to observed severe side effects.[2] One way to overcome this problem is to control the MMPs by manipulating MMP-regulatory factors.

Here, we demonstrate that Plg deficiency, either as a genetic knockout or by pharmacological inducement using YO-2, an active-center-directed inhibitor of Plm,[10] inhibits MMP-9-dependent T-cell lymphoma growth. Using in vivo models, we provide compelling evidence that Plg regulates T-cell lymphoma growth and the influx of myeloid cells into the lymphoma niche in an MMP-9-dependent manner. Thus, Plm is a novel therapeutic target for treatment of certain lymphoid malignancies.

Materials and methods

Mice

WT (Plg⁺/⁺) and Plg⁻/⁻ mice[11] and WT (MMP-9⁺/⁺) and MMP-9⁻/⁻ mice (kindly provided by Zena Werb, University of California San Francisco, USA and Leif R Lund, University of Copenhagen, Denmark) were obtained by heterozygous breeding of mice backcrossed into a C57BL/6J background. For the

in vivo experiments, all mice were inoculated at age 6–8 weeks. Animal procedures were approved by the Animal Care Committee of Juntendo University. C57BL/6 mice were purchased from SLC, Inc. (Shizuoka, Japan).

Cell lines

B6RV2 cells[12] were cultured in Iscove's modified Dulbecco's medium (Invitrogen, Carlsbad, CA, USA) containing 10% fetal bovine serum (MP Biomedicals, Aurora, OH, USA), penicillin and streptomycin (WAKO, Osaka, Japan). RMA and FBL3 cells were cultured in RPMI medium 1640 (SIGMA, St Louis, MO, USA) containing 10% fetal bovine serum. EL4T cell lymphoma cells were expanded in RPMI medium 1640 containing 10% fetal bovine serum supplemented with 2 mM L-glutamine, 0.05 mM 2-mercaptoethanol (Invitrogen), penicillin and streptomycin.

In vivo T-cell lymphoma model

The dorsal skin of mice was shaved 1 day before inoculation. The following day, washed lymphoma cells, exceeding 95% cell viability by trypan blue dye exclusion were inoculated into mice (10^8 B6RV2, 5×10^7 FBL3 or 6×10^5 RMA cells per mouse into the dorsal subcutis). Some mice received 10^8 B6RV2 intravenous. Lymphoma length, width and height were measured. Lymphoma volume was calculated as ((length) × (width) × (height)). Mice were injected daily with YO-2 or carboplatin or mutant tPA (Eizai, Tokyo, Japan) for the first 5 days at the concentration of 3.8 or 50 or 10 mg/kg body weight, respectively. White blood cells were measured using an automatic blood cell counter MEK-6308 (Nihon Kohden Co., Tokyo, Japan). Survival was monitored.

In vivo CD11b blocking experiment

Mice were inoculated with 10^8 B6RV2 cells subcutaneously and treated with/without 500 μg anti-CD11b (clone 5C6), or with control immunoglobulin G on days 1, 3, 5 and 7. T-cell lymphoma volume was then determined.

Fluorescence-activated cell sorting (FACS)

Harvested T-cell lymphoma tissue was minced. Cell pellets were blocked with an Fc block (clone 2.4G2, BD Pharmingen, San Diego, CA, USA), washed and stained with anti-CD45-Pacific Blue (clone 30–F11, BioLegend, San Diego, CA, USA), anti-vascular endothelial growth factor (VEGF) receptor-1 (R1)-biotin (clone MF-1, ImClone Systems, New York, NY, USA), anti-F4/80-FITC (BM8, BioLegend), anti-Gr-1-FITC (clone RB6-8C5, BD Pharmingen), anti-CD11b-PE (clone M1/70), BD Pharmingen) or anti-CXCR4-FITC (clone 2B11/CXCR4, BD Pharmingen). Cells stained with VEGF-R1-biotin were washed and then incubated with Streptavidin-APC (BD Pharmingen) at 4 °C for 15 min. Dead cells were excluded using propidium iodide staining. Cells were analyzed using a FACSAria machine (BD Biosciences, San Jose, CA, USA).

Immunohistochemistry

Acetone-fixed frozen T-cell lymphoma sections were stained for F4/80. In brief, sections were blocked with the Biotin-Blocking System (Dako, Carpinteria, CA, USA) and 5% goat serum (VECTOR, Burlingame, CA, USA), and incubated overnight at 4 °C with the anti-F4/80 antibody (Ab) (10 μg/ml; clone C1:A3-1, Serotec, Oxford, UK). Rat immunoglobulin G (clone 141 945, R&D Systems Inc., Minneapolis, MN, USA) served as a negative control. Next, endogenous peroxidase was blocked using 3%

H_2O_2 in methanol followed by biotin-labeled rabbit anti-rat immunoglobulin G Ab (clone CLCC40015, Cedarlane Laboratories, Hornby, ON, Canada) and a horseradish peroxidase or Alexa594-conjugated Streptavidin Ab. DAB (WAKO or Alexa 594, Molecular Probes, Eugene, OR, USA), developed sections were counterstained with hematoxylin. Sections were stained with an anti-CD31 Ab (clone: T-2001, BMA, Rockland, ME, USA) followed by a biotin-labeled rabbit anti-rat immunoglobulin G Ab (clone CLCC40015, Cedarlane Laboratories) and an Alexa594-conjugated Streptavidin Ab (Alexa 594, Molecular Probes).

Reverse transcription-PCR

RNA was extracted using Trizol (Invitrogen), followed by a DNase (Nippon Gene, Tokyo, Japan) reaction. The purity and integrity of the extracted RNA was checked spectroscopically and by gel electrophoresis before use. cDNA was generated using a High Capacity cDNA Archive Kit (Applied Biosystems, Foster City, CA, USA) and was stored at −80 °C. PCR mixtures (12 μl final volume) contained 6 μl of a 2 × PCR master mix (Promega, Heidelberg, Germany), 1 μl of template cDNA and primers (at a final concentration of 1 μM). Reaction mixtures were incubated in a thermocycler. The respective forward and reverse murine primers used for reverse transcription-PCR were as follows: β-actin: 5′-GCTTCTTTGCAGCTCCTTCGT-3′ and 5′-CCAGCGCAGCGATATCG-3′; transforming growth factor-β_1: 5′-TCCCGTGGCTTCTAGTGCTG-3′ and 5′-ATTTTAATCTCTG CAAGCGCA-3′, VEGF-A: 5′-CAGGCTGCTGTAACGATGAA-3′ and 5′-AATGCTTTCTCCGCTCTGAA-3′; c-Kit: 5′-ATCCCGACT TTGTCAGATGG-3′, 5′-AAG GCCAACCAGGAAAAGTT-3′.

Enzyme-linked immunosorbent assay

Mice were bled retro-orbitally using heparin-coated glass capillaries. MMP-9, VEGF-A, and Kit ligand (KitL) plasma levels were measured using the commercially available enzyme-linked immunosorbent assay kits (R&D Systems Inc.).

Statistics

Data are reported as the mean ± s.e.m. Student *t*-tests were performed. $P < 0.05$ were considered significant.

Results

Plg and MMP-9 are required for T-cell lymphoma growth

To assess the role of Plg in T-cell lymphoma growth, T-cell lymphoma cells were inoculated subcutaneously into Plg$^{−/−}$ and WT mice. B6RV2, RMA and FBL3T cell lymphoma growth was delayed in Plg$^{−/−}$ mice compared with WT mice (Figures 1a–c). Daily recombinant tissue-type Plg activator administration accelerated B6RV2 lymphoma growth in WT, but not in Plg$^{−/−}$ mice (Figure 1a). We previously demonstrated that Plg can upregulate MMP-9 during tissue regeneration.[4] Plasma MMP-9 levels increased over time in WT, but not in Plg$^{−/−}$ B6RV2T cell lymphoma-bearing mice (Figure 1d). To understand the role of MMP-9 in T-cell lymphoma growth, T-cell lymphoma cells were inoculated subcutaneously into MMP-9$^{−/−}$ and WT mice. Lymphoma growth of B6RV2, RMA and FBL3T lymphoma cells (Figures 1e–g) was delayed in MMP-9$^{−/−}$ mice compared with WT mice. Overall, these studies provide solid evidence that Plg and MMP-9 have a role in T-cell lymphoma growth.
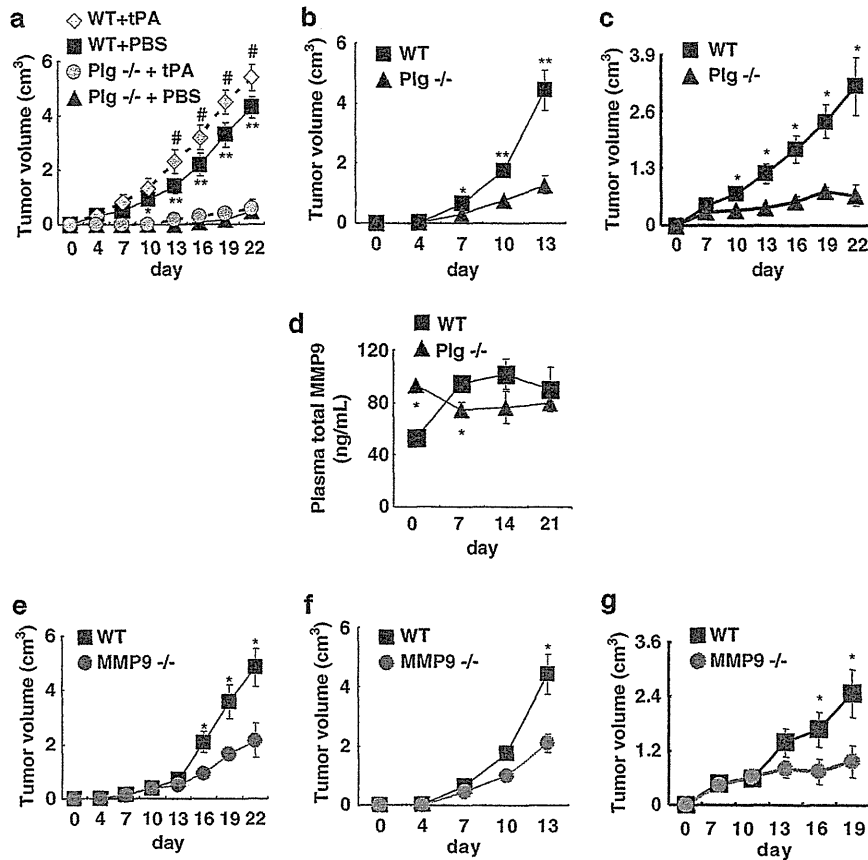
Figure 1 Plg and MMP-9 are required for lymphoma growth. (a–c) WT and Plg$^{-/-}$ mice were injected subcutaneously with B6RV2 or RMA cells or FBL3 cells. (a) B6RV2 lymphoma growth was determined in WT and Plg$^{-/-}$ mice treated daily with/without recombinant tissue-type Plg activator (tPA) for 5 days ($n=6$ for tPA-treated WT mice; $n=10$ for WT mice; $n=6$ for tPA-treated Plg$^{-/-}$ mice; $n=11$ for Plg$^{-/-}$ mice; *$P<0.05$ and **$P<0.01$ comparing WT with Plg$^{-/-}$ mice; #$P<0.05$ comparing tPA-treated WT with WT mice). (b) RMA lymphoma growth was determined in WT and Plg$^{-/-}$ mice ($n=5$; *$P<0.05$ comparing WT with Plg$^{-/-}$ mice). (c) FBL3 lymphoma growth was determined in WT and Plg$^{-/-}$ mice ($n=4$; *$P<0.05$ comparing WT with Plg$^{-/-}$ mice). (d) Plasma samples derived from B6RV2 lymphoma-bearing WT and Plg$^{-/-}$ mice were analyzed for total MMP-9 levels by enzyme-linked immunosorbent assay ($n=3$; *$P<0.05$). (e–g) WT and MMP-9$^{-/-}$ mice were injected subcutaneously, with murine B6RV2 or RMA cells. (e) B6RV2 lymphoma growth was determined ($n=9$ for WT mice; $n=5$ for MMP-9$^{-/-}$ mice; *$P<0.05$ comparing WT with MMP-9$^{-/-}$ mice). (f) RMA lymphoma growth was determined ($n=8$ for WT mice; $n=4$ for MMP-9$^{-/-}$ mice; *$P<0.05$ comparing WT with MMP-9$^{-/-}$ mice). (g) FBL3 lymphoma growth was determined ($n=5$; *$P<0.05$ comparing WT with MMP-9$^{-/-}$ mice).

Plg and MMP-9 are required for myeloid cell infiltration during T-cell lymphoma growth

We next addressed the potential role of Plg and MMP-9 in myeloid cell infiltration. Lymphoma cells were inoculated subcutaneously into Plg$^{-/-}$, MMP-9$^{-/-}$ and WT mice and then infiltrating hematopoietic cells were identified by FACS in minced lymphoma tissues using cell markers known to promote angiogenesis or tumorigenesis: CD45$^+$VEGF-R1$^+$CXCR4$^+$ (hemangiocytes),[13] CD45$^+$CD11b$^+$Gr-1$^+$ (myelomonocytic cells)[14] and CD45$^+$CD11b$^+$F4/80$^+$ (macrophages and eosinophils).[15] CD45$^+$CD11b$^+$F4/80$^+$ cells were the most abundant infiltrating cells in WT lymphoma-bearing mice, and their frequency was reduced in Plg$^{-/-}$ and MMP-9$^{-/-}$ B6RV2 lymphoma-bearing mice (Figures 2a and b), and in Plg$^{-/-}$ RMA T-cell lymphoma-bearing mice (Figure 2c). Infiltration of CD45$^+$CD11b$^+$Gr-1$^+$ cells was reduced only in Plg$^{-/-}$ lymphoma (Supplementary Figure S1) All other tested cell populations showed a low frequency of infiltration (<1%) and showed no difference between T-cell lymphoma tissue derived from Plg$^{-/-}$ or MMP-9$^{-/-}$ and that from WT mice (data not shown). The number of infiltrating F4/80$^+$ myeloid cells was reduced in B6RV2 lymphoma tissues derived from Plg$^{-/-}$ and MMP-9$^{-/-}$ compared with those derived from WT mice (Figures

2d and e) and in Plg$^{-/-}$ RMA T-cell lymphoma tissue (Figure 2f), indicating that CD45$^+$CD11b$^+$F4/80$^+$ myeloid cell infiltration into T-cell lymphomas is driven by host-derived Plg and MMP-9.

Plm inhibitor blocks lymphoma growth by suppressing MMP-9-dependent CD11b$^+$F4/80$^+$ cell recruitment

The in vivo results above raised the hypothesis that Plg regulates T-cell lymphoma growth via MMP-9. To test this hypothesis, we evaluated the effect of the Plm inhibitor YO-2 against T-cell lymphoma growth. Daily injections of YO-2 reduced T-cell lymphoma growth in WT mice (Figure 3a), but did not further decrease lymphoma growth in Plg$^{-/-}$ mice (Figure 3a). We compared the T-cell lymphoma growth-controlling effect of YO-2 with the antitumor drug carboplatin (Figure 3b) using the B6RV2T cell lymphoma murine model. Similar tumor growth retardation was observed in the YO-2-treated group compared with the carboplatin-treated group. YO-2 treatment in combination with carboplatin did not further inhibit tumor growth.

Interestingly, YO-2 treatment did not further decrease lymphoma growth in MMP-9$^{-/-}$ mice (Figure 3c). Plasma MMP-9 level elevation observed in WT lymphoma-bearing mice was blocked in YO-2-treated lymphoma-bearing WT mice
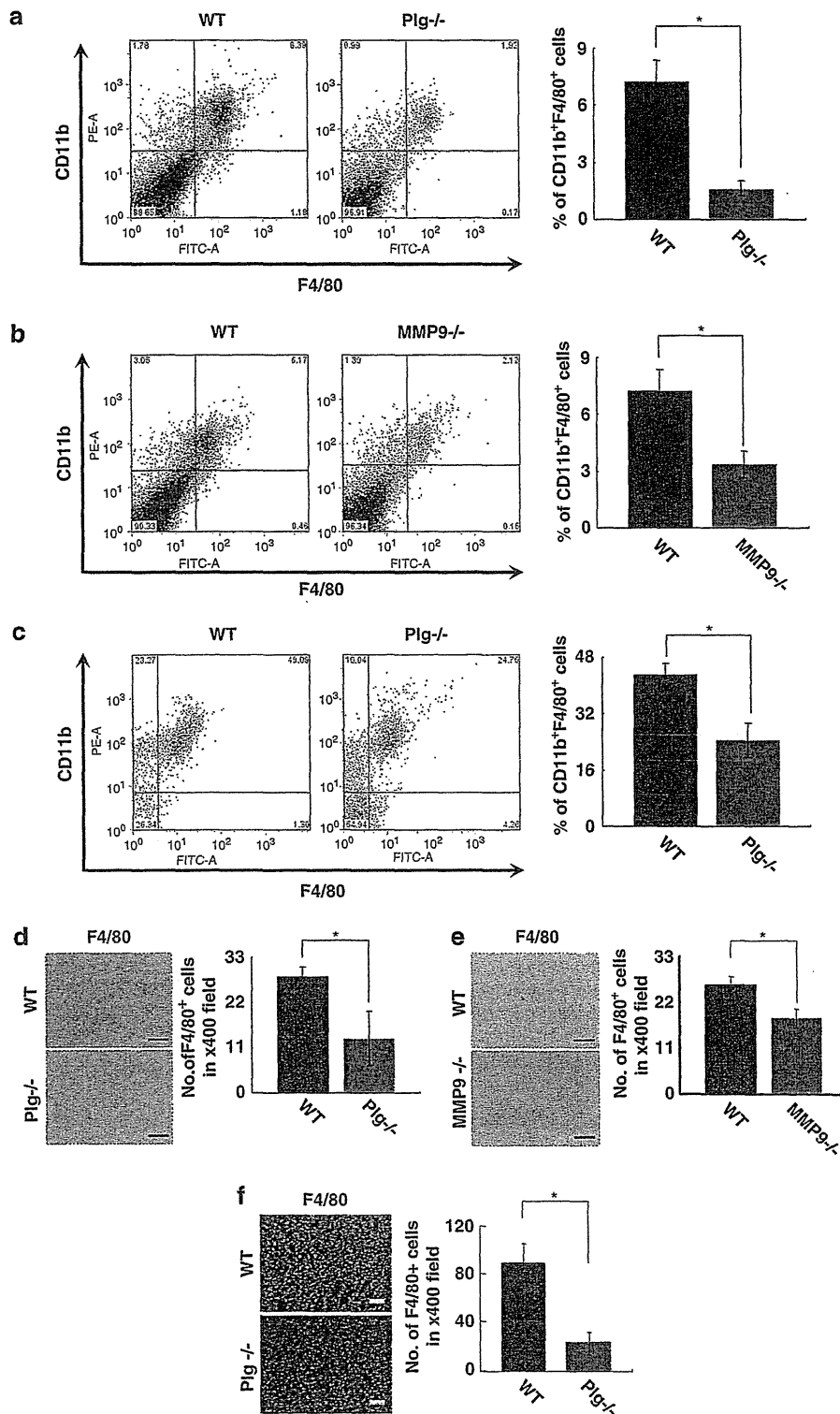
Figure 2 Plg and MMP-9 are required for myeloid cell infiltration during lymphoma growth. (a, b) B6RV2 lymphoma tissues were obtained from WT, Plg$^{-/-}$ and MMP-9$^{-/-}$ mice on day 7 after cell inoculation. The number of CD11b$^+$F4/80$^+$ cells was determined by FACS (a) in minced WT and Plg$^{-/-}$ lymphoma tissue derived from B6RV2 lymphoma ($n = 19$ for WT and $n = 10$ for Plg$^{-/-}$-derived cells; *$P < 0.05$) and (b) in minced WT and MMP-9$^{-/-}$ lymphoma tissue derived from B6RV2 lymphoma ($n = 19$ for tissue-derived cells from WT and $n = 9$ for MMP-9$^{-/-}$mice; *$P < 0.05$). (c) RMA lymphoma tissues were obtained from WT and Plg$^{-/-}$ mice on day 6 after cell inoculation. The number of CD11b$^+$F4/80$^+$ cells in minced WT and Plg$^{-/-}$ RMA lymphoma tissue was determined by FACS ($n = 3$ for WT and $n = 3$ for Plg$^{-/-}$-derived cells; *$P < 0.05$). (d) The number of F4/80$^+$ cells per high power field is decreased within Plg$^{-/-}$ compared with WT B6RV2 lymphoma tissue as determined by immunohistochemical staining on day 7 ($n = 3$; *$P < 0.05$). Arrows indicate F4/80$^+$ cells. Scale bar $= 100$ μm. (e) Immunohistochemical staining of day 7 tissues of F4/80$^+$ cells in B6RV2 lymphoma tissue. The number of F4/80$^+$ cells per high power field was assessed ($n = 6$; *$P < 0.05$). Scale bar $= 100$ μm. (f) Immunohistochemical staining of day 7 tissues of F4/80$^+$ cells in RMA lymphoma tissue. The number of F4/80$^+$ cells per high power field was assessed ($n = 3$ for WT and $n = 4$ for MMP-9$^{-/-}$-derived lymphoma tissue; *$P < 0.05$). Scale bar $= 100$ μm.
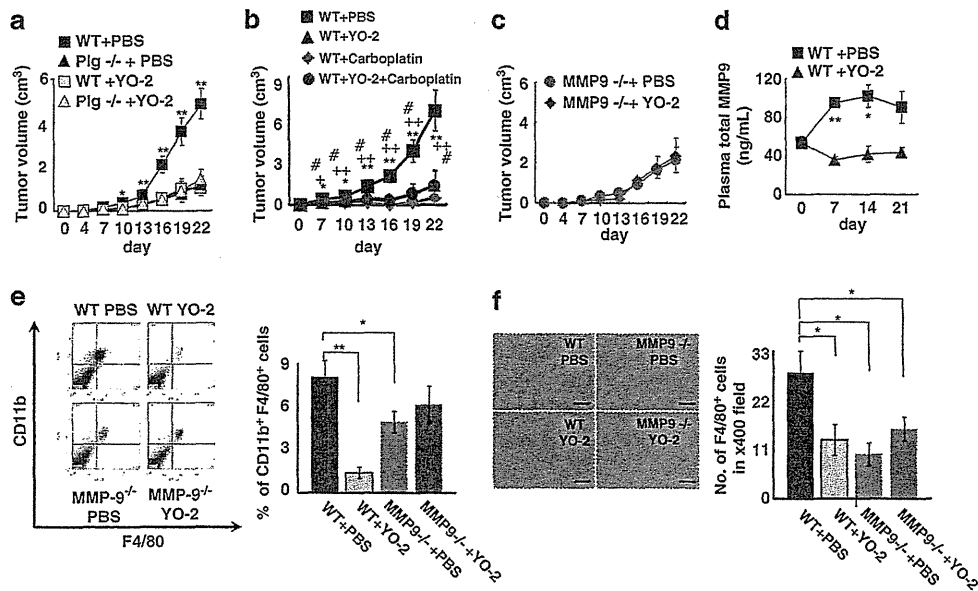
Figure 3 Plm inhibitor blocks lymphoma growth by suppressing MMP-9-dependent CD11b$^+$F4/80$^+$ cell recruitment. (a–c) MMP-9$^{-/-}$ and Plg$^{-/-}$ and corresponding WT control mice were injected subcutaneously with B6RV2 cells and treated intra-peritoneal with/without Plm inhibitor YO-2. (a–c) Lymphoma volume was measured at different time points after cell inoculation (a): $n = 9$ for WT mice; $n = 10$ for YO-2-treated WT mice; $n = 9$ for MMP-9$^{-/-}$ mice; $n = 10$ for YO-2-treated MMP-9$^{-/-}$ mice; $n = 5$ for YO-2-treated Plg$^{-/-}$ mice; *$P < 0.05$ and **$P < 0.01$ comparing WT with YO-2-treated WT mice, (b, c); $n = 4$ *$^{+\#}P < 0.05$ and ** $^{+\#\#}P < 0.01$). (d) ELISA assay for measurement of total MMP-9 levels in plasma samples obtained from WT mice treated with or without YO-2 ($n = 3$; *$P < 0.05$ and **$P < 0.01$ comparing WT with YO-2-treated WT mice). (e, f) MMP-9$^{-/-}$ and WT mice were injected subcutaneously with B6RV2 cells and treated intra-peritoneal with/without Plm inhibitor YO-2. (e) On day 7, the number of CD11b$^+$F4/80$^+$ cells was determined by FACS within crushed lymphoma tissues of the mice ($n = 11$ for WT and $n = 6$ for YO-2-treated WT-derived cells; $n = 11$ for MMP-9$^{-/-}$ and $n = 8$ for YO-2-treated MMP-9$^{-/-}$-derived cells; *$P < 0.05$ and **$P < 0.01$) (f) The density of F4/80$^+$ cells was quantified in day 7 lymphoma tissues ($n = 4$ for WT and $n = 7$ for YO-2-treated WT-derived lymphoma tissue; *$P < 0.05$ and **$P < 0.01$, and $n = 4$ for MMP-9$^{-/-}$ or $n = 8$ for YO-2-treated MMP-9$^{-/-}$-derived lymphoma tissue). Scale bar $= 100\,\mu$m.

(Figure 3d). These results indicate that B6RV2 lymphoma growth is controlled by Plg via MMP-9, and YO-2 can block B6RV2 lymphoma growth. This conclusion suggests that Plg is a direct therapeutic target to tackle lymphoma.

Plg/Plm is the main enzyme among the fibrinolytc system. To test whether other fibrinolytic inhibitors are also applicable to the treatment of T-cell lymphoma, B6RV2-bearing mice were treated with tranexamic acid (TA), a synthetic derivative of the amino-acid lysine, which exerts its anti-fibrinolytic effect through the reversible blockade of lysine binding sites on Plg molecules. TA caused T-cell lymphoma growth retardation, but this effect did not reach significance (Supplementary Figure S2). TA is a drug that blocks fibrinolysis although it does not inhibit the enzymatic activity of Plm.[16] This indicates that Plg regulate T-cell lymphoma growth independently of its fibrinolytic function.

YO-2 treatment reduced the tissue infiltration of CD45$^+$CD11b$^+$F4/80$^+$ myeloid cells, and the infiltration of F4/80$^+$ cells in WT, but not in MMP-9$^{-/-}$ lymphoma-bearing mice, respectively (Figures 3e and f). Additionally, the infiltration of CD11b$^+$Gr-1$^+$ cells was inhibited in WT mice but not in MMP-9$^{-/-}$ mice by YO-2 treatment (Supplementary Figure S1). To identify the hematopoietic cell types within the CD45$^+$CD11b$^+$F4/80$^+$ cells derived from T-cell lymphoma tissues, we sorted CD45$^+$CD11b$^+$F4/80$^+$ cells according to their sideward light scatter (SSC) into SSC^{high} and SSC^{low} cells using FACSAria. The SSC^{high} fraction consisted of eosinophils, whereas the SSC^{low} fraction contained mainly monocytes (Figure 4a). We observed delayed tumor growth in Plg$^{-/-}$ mice injected with B6RV2 or RMA T-cell T-cell lymphoma cells, but not in mice inoculated with the EL4T cell T-cell lymphoma, Lewis lung carcinoma or B16 melanoma cells (data not shown).

We mainly found eosinophils in crushed tumor tissues of B6RV2 and RMA, and monocytes in tumor tissues established using EL4, B16 and Lewis lung carcinoma cells (Figure 4b). Anti-CD11b treatment reduced T-cell lymphoma growth in WT mice and no significant further T-cell lymphoma growth retardation was observed in anti-CD11b-treated Plg$^{-/-}$ mice (Figure 4c).

In mice challenged intravenously with lymphoma cells, treatment with Plm inhibitor YO-2 prolonged the survival compared with the phosphate-buffered saline-treated group (Figure 4d), although the white blood cell counts were not significantly different between both groups (Figure 4e). Indeed, treatment of YO-2 in vitro did not affect lymphoma cell proliferation (data not shown). These data indicate that YO-2 improved the survival of lymphoma-inoculated mice not by suppressing the proliferation of B6RV2 cells but by modulating the local lymphoma microenvironment. Taken together, these results suggest that YO-2, a specific Plm inhibitor, can reduce T-cell lymphoma growth through regulating MMP-9-dependent CD11b$^+$/F4/80$^+$ myeloid cell recruitment.

Plm inhibitor blocks cytokine increase during T-cell lymphoma growth

Protease–cytokine interactions are important in the remodeling of the T-cell lymphoma microenvironment in T-cell lymphoma growth. Recent reports have indicated that tumor-infiltrating myeloid cells are a source for local cytokine release into the tumor microenvironment in vivo and related to tumor malignancy.[17,18] We examined T-cell lymphoma growth-associated cytokine expression in FACS-isolated CD45$^+$CD11b$^+$F4/80$^+$ cells from B6RV2-bearing T-cell lymphoma tissues (Figure 5a). Tumor-infiltrating CD45$^+$CD11b$^+$F4/80$^+$ cells expressed
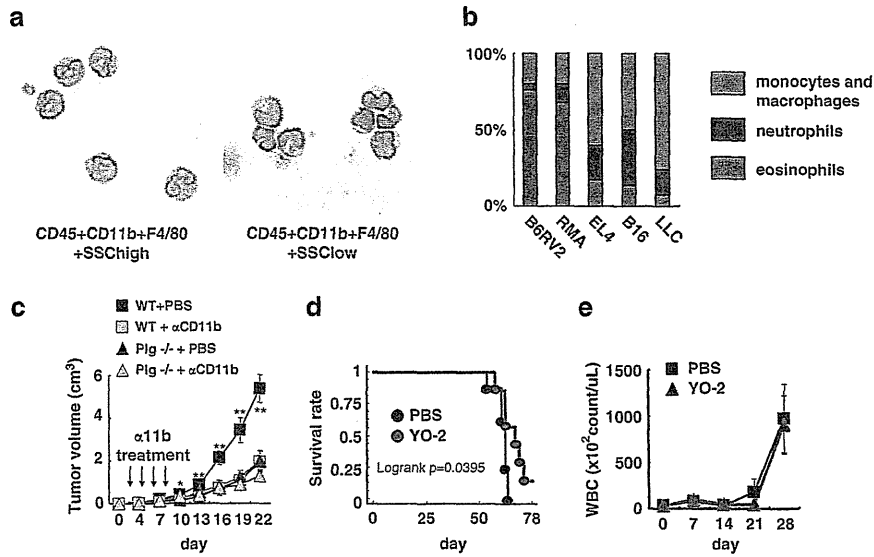
Figure 4 Lymphoma-derived CD45$^+$CD11b$^+$F4/80$^+$ cells consisted of eosinophils. (a, b) Lymphoma-derived CD45$^+$CD11b$^+$F4/80$^+$ cells were gated into SSC^{high} and SSC^{low} cells and were isolated by FACSAria. The SSC^{high} fraction consisted of eosinophils, whereas the SSC^{low} fraction mainly contained monocytes as visualized on May Grunwald-stained slides. (b) Relative contribution of different hematopoietic cell types within the tumor-infiltrating CD45$^+$CD11b$^+$ cell population isolated from various murine tumors. ($n = 3$). (c) B6RV2-injected Plg$^{-/-}$ and WT mice were treated with anti-CD11b or control antibodies ($n = 3$; $^*P < 0.05$; $^{**}P < 0.01$). Tumor volume was measured. (d) WT mice were injected intravenously with B6RV2 followed by treatment with phosphate-buffered saline or YO-2 and survival rate was observed. Statistic analysis using log rank test showed P-value of 0.0395 ($n = 7$). (e) WT mice were injected intravenously with B6RV2 followed by treatment with PBS (phosphate-buffered saline) or YO-2. White blood cell (WBC) count was measured ($n = 4$).
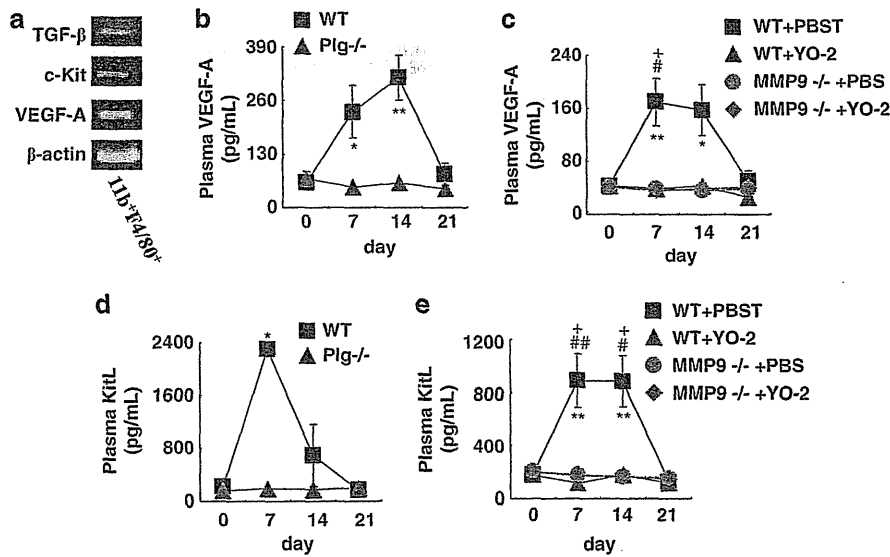

Figure 5 Plm inhibitor blocks cytokine increase during lymphoma growth. (a) CD45$^+$CD11b$^+$F4/80$^+$ cells were sorted out from B6RV2 lymphoma-bearing WT mice and cDNA was obtained. Reverse transcription-PCR was performed for several cytokines and receptors. The result was confirmed by repeating once. (b, c) ELISA assay of VEGF-A in plasma samples: (b); $n = 3$; $^*P < 0.05$ and $^{**}P < 0.01$; (c); $n = 3$; $^*P < 0.05$ and $^{**}P < 0.01$ comparing PBS-treated WT with YO-2-treated WT mice; $^\#P < 0.05$ comparing PBS-treated WT with PBS-treated MMP-9$^{-/-}$ mice; $^+P < 0.05$ comparing PBS-treated WT with YO-2-treated MMP-9$^{-/-}$ mice. (d, e) ELISA assay of KitL in plasma samples: (d) $n = 3$; $^*P < 0.05$, (e); $n = 3$; $^{**}P < 0.01$ comparing PBS-treated WT with YO-2-treated WT mice; $^\#P < 0.05$ and $^{\#\#}P < 0.01$ comparing PBS-treated WT with PBS-treated MMP-9$^{-/-}$ mice; $^+P < 0.05$ comparing PBS-treated WT with YO-2-treated MMP-9$^{-/-}$ mice.

transforming growth factor-β 1, VEGF-A and c-Kit. The former factors are known to influence the survival and proliferation of T-cell lymphoma cells.[17]

Plg or MMPs can liberate VEGF-A from extracellular matrix stores.[19] Augmented plasma VEGF-A levels were observed in T-cell lymphoma-bearing WT, but not in Plg$^{-/-}$ mice (Figure 5b), in YO-2-treated WT mice, nor in MMP-9$^{-/-}$ mice with or without YO-2 treatment (Figure 5c). VEGF-A is a well-known angiogenic factor. But surprisingly, Plg deficiency

did not result in reduced vessel density in B6RV2T cell lymphoma tissues when compared with WT controls (Supplementary Figure S3), implying that the reduced T-cell lymphoma growth was not due to impaired angiogenesis. It has been shown that VEGF-A induces hematopoietic cell mobilization and myeloid cell differentiation.[20,21] KitL also induces myeloid cell differentiation.[22]

Plasma KitL levels were increased in T-cell lymphoma-bearing WT, but not in Plg$^{-/-}$ mice (Figure 5d), but did not

338

rise in T-cell lymphoma-bearing mice with drug- or genetically-induced Plg deficiency, with MMP-9 deficiency with or without YO-2 treatment (Figure 5e). Interestingly, the peak of infiltration of CD11b$^+$F4/80$^+$ cells into T-cell lymphoma tissues coincided with peak plasma KitL levels in T-cell lymphoma-bearing WT mice (data not shown). Lymphoma patients show abnormal plasma levels of cytokines produced primarily by lymphoma cells or secondarily by stromal cells.[23] Myeloid cells can provide proangiogenic factors such as VEGF-A and MMP-9.[24]

VEGF-A can be liberated from extracellular matrix stores after Plg or MMP activation.[19] Our data demonstrate that Plg activation during lymphoma growth controls plasma VEGF-A levels via MMP-9 modulation. Indeed, we showed that VEGFR1 was required for myeloid cell recruitment into B6RV2 lymphoma tissues in vivo.[25] We have shown that activation of MMP-9 by Plm can expand the myeloid cell pool and mobilize pro-angiogenic myeloid cells, a process dependent on VEGF-A and KitL.[4] Here, our findings indicate that Plm activation during T-cell lymphoma growth increases plasma VEGF-A and KitL levels and recruits CD11b$^+$F4/80$^+$ cells into T-cell lymphoma tissues.

Discussion

The tumor microenvironment including immune cells, fibrosis and angiogenesis can influence the survival of lymphoma patients after treatment.[26] Our study provides in vivo evidence that Plg regulates T-cell lymphoma growth upstream of MMP-9, and controls both the infiltration of CD45$^+$CD11b$^+$F4/80$^+$ into T-cell lymphomas and the release of stromal cell-associated growth factors. We propose that targeted inhibition of Plg is a new therapeutic approach that can control T-cell lymphoma growth by modulating the T-cell lymphoma microenvironment.

We showed that T-cell lymphoma growth in a T-cell lymphoma model was retarded in MMP-9$^{-/-}$ mice and that Plm inhibitors failed to further decrease the already low T-cell lymphoma growth in MMP-9-deficient mice. Other protumorgenic targets of Plg aside from MMP-9 are conceivable, for example, MMP-3, as Plm also activate pro-MMP-1, pro-MMP-3 and pro-MMP13 [refs 27,28] or pro-tumorgenic growth factors and cytokines such as basic fibroblast growth factor.[29]

A study using a spontaneous T-cell lymphoma model demonstrated that MMP-9 deficiency in lymphoma cells resulted in a drop in survival time caused by increased tumor metastasis.[30] Further studies will be necessary to unravel the role of Plg and MMP in the invasion and metastasis of T-cell lymphoma cells.

As previously stated, Plm induces fibrinolysis.[2] Recently, tumor growth dependence on fibrinogen has been linked to the anatomic location of the tumor.[31] Tumor growth of Lewis lung carcinoma was sustained in Plg$^{-/-}$ mice when transplanted into the dorsal skin but was suppressed in the footpad, where vaso-occlusive thrombi occurrence limited tumor blood supply. Fibrinogen deficiency restored tumor growth in footpad-transplanted Plg$^{-/-}$ mice. How is T-cell lymphoma growth controlled by Plm/the fibrinolytic system? Plm deficiency, either genetically-induced (Plg$^{-/-}$ mice) or drug-induced (treatment with YO-2, an inhibitor of Plm), blocked T-cell lymphoma growth, indicating that Plg activation was required for T-cell lymphoma growth. YO-2 treatment inhibited T-cell lymphoma growth as efficiently as genetic deletion of Plg. Although YO-2 blocked the T-cell lymphoma growth, TA administration to the T-cell lymphoma model did not cause T-cell lymphoma growth delay (Supplementary Figure S2). TA is a drug that blocks fibrinolysis, but can accelerate Plm formation in vitro.[16]

We therefore proposed that T-cell lymphoma growth retardation was due to the action of Plm, rather than to that of fibrinogen. Further studies will be necessary to prove this hypothesis.

Infiltrating innate immune cells support lymphoma cell survival and/or proliferation and correlate with a poor prognosis.[32] We show that CD45$^+$CD11b$^+$F4/80$^+$ myeloid cell influx requires the presence of both MMP-9 and Plm whereas infiltration of CD11b$^+$Gr-1$^+$ myeloid cells into T-cell lymphoma tissues is Plg dependent, but is independent of MMP-9. The importance of CD11b$^+$ cells for T-cell lymphoma growth was confirmed in the studies using neutralizing antibodies against CD11b. T-cell lymphoma growth was inhibited in WT mice and could not be further blocked in Plg$^{-/-}$ mice, indicating that the role of Plg for T-cell lymphoma growth was driven by its ability to regulate CD11b$^+$ cell migration. A role of Plg in CD45$^+$ cell migration into the medial layer of allografted vascular tissue in graft vascular disease model has been reported.[33]

Cytokines and chemokines released from tumor cells can regulate the influx of hematopoietic cells. Plg-dependent tumor inhibition was observed in tumors in which a high rate of infiltrating eosinophils had been detected. We observed increased KitL levels in lymphoma-bearing mice, which was blocked in Plg-deficient mice. KitL can recruit c-kit receptor-positive eosinophils.[34] Eotaxin, a potent eosinophil chemotactic factor promotes eosinophil transmigration via the activation of the Plg–Plm system[35] Further studies will be necessary to understand whether these or other factors released from tumor cells have a role for the observed impaired influx of myeloid cells into tumors after Plm inhibition. The role of eosinophils is controversial in different types of malignancies as both growth promoting and inhibitory effects had been described.[36] Further studies will be needed to understand the role of eosinophils in T-cell lymphoma and to establish a role for Plg in the regulation of other eosinophilia-associated diseases. In our model, CD45$^+$CD11b$^+$F4/80$^+$ cells expressed cytokines such as VEGF-A and transforming growth factor-β. These factors are known to accelerate lymphoma growth.[37] These studies support our findings that myeloid cell infiltration is dependent on the activation of the Plg/MMP-9 pathway. Furthermore, multiple reports have shown that myeloid cells mediate key steps of tumor progression.[38]

In conclusion, we show that the Plg/MMP-9 pathway can regulate T-cell lymphoma growth and accelerate the recruitment of T-cell lymphoma growth supportive CD45$^+$CD11b$^+$F4/80$^+$ myeloid cells into T-cell lymphoma tissues. Therefore, targeting the Plg/MMP-9 pathway (for example, using YO-2) should offer a new approach for therapeutic intervention in lymphoid malignancy.

Conflict of interest

The authors declare no conflict of interest.

References

1 Huber K, Kirchheimer JC, Sedlmayer A, Bell C, Ermler D, Binder BR. Clinical value of determination of urokinase-type plasminogen activator antigen in plasma for detection of colorectal cancer: comparison with circulating tumor-associated antigens CA 19-9 and carcinoembryonic antigen. Cancer Res 1993; 53: 1788–1793.

2 Dano K, Behrendt N, Hoyer-Hansen G, Johnsen M, Lund LR, Ploug M et al. Plasminogen activation and cancer. Thromb Haemost 2005; 93: 676–681.

3 Thomas GT, Lewis MP, Speight PM. Matrix metalloproteinases and oral cancer. Oral Oncol 1999; 35: 227–233.

4 Heissig B, Lund LR, Akiyama H, Ohki M, Morita Y, Romer J et al. The plasminogen fibrinolytic pathway is required for hematopoietic regeneration. Cell Stem Cell 2007; 1: 658–670.

5 Hazar B, Polat G, Seyrek E, Bagdatoglglu O, Kanik A, Tiftik N. Prognostic value of matrix metalloproteinases (MMP-2 and MMP-9) in Hodgkin's and non-Hodgkin's lymphoma. Int J Clin Pract 2004; 58: 139–143.

6 Johansson M, Denardo DG, Coussens LM. Polarized immune responses differentially regulate cancer development. Immunol Rev 2008; 222: 145–154.

7 Ruan J, Hajjar K, Rafii S, Leonard JP. Angiogenesis and antiangiogenic therapy in non-Hodgkin's lymphoma. Ann Oncol 2009; 20: 413–424.

8 Van Lint P, Libert C. Chemokine and cytokine processing by matrix metalloproteinases and its effect on leukocyte migration and inflammation. J Leukoc Biol 2007; 82: 1375–1381.

9 Coussens LM, Tinkle CL, Hanahan D, Werb Z. MMP-9 supplied by bone marrow-derived cells contributes to skin carcinogenesis. Cell 2000; 103: 481–490.

10 Okada Y, Tsuda Y, Wanaka K, Tada M, Okamoto U, Okamoto S et al. Development of plasmin and plasma kallikrein selective inhibitors and their effect on M1 (melanoma) and HT29 cell lines. Bioorg Med Chem Lett 2000; 10: 2217–2221.

11 Bugge TH, Flick MJ, Daugherty CC, Degen JL. Plasminogen deficiency causes severe thrombosis but is compatible with development and reproduction. Genes Dev 1995; 9: 794–807.

12 Nakayama E, Uenaka A, Stockert E, Obata Y. Detection of a unique antigen on radiation leukemia virus-induced leukemia B6RV2. Cancer Res 1984; 44: 5138–5144.

13 Jin DK, Shido K, Kopp HG, Petit I, Shmelkov SV, Young LM et al. Cytokine-mediated deployment of SDF-1 induces revascularization through recruitment of CXCR4+ hemangiocytes. Nat Med 2006; 12: 557–567.

14 Shojaei F, Wu X, Malik AK, Zhong C, Baldwin ME, Schanz S et al. Tumor refractoriness to anti-VEGF treatment is mediated by CD11b+Gr1+ myeloid cells. Nat Biotechnol 2007; 25: 911–920.

15 Lin EY, Li JF, Gnatovskiy L, Deng Y, Zhu L, Grzesik DA et al. Macrophages regulate the angiogenic switch in a mouse model of breast cancer. Cancer Res 2006; 66: 11238–11246.

16 Longstaff C. Studies on the mechanisms of action of aprotinin and tranexamic acid as plasmin inhibitors and antifibrinolytic agents. Blood Coagul Fibrinolysis 1994; 5: 537–542.

17 Zhao WL, Mourah S, Mounier N, Leboeuf C, Daneshpouy ME, Legres L et al. Vascular endothelial growth factor-A is expressed both on lymphoma cells and endothelial cells in angioimmuno-blastic T-cell lymphoma and related to lymphoma progression. Lab Invest 2004; 84: 1512–1519.

18 Kadin ME, Cavaille-Coll MW, Gertz R, Massague J, Cheifetz S, George D. Loss of receptors for transforming growth factor beta in human T-cell malignancies. Proc Natl Acad Sci USA 1994; 91: 6002–6006.

19 Heissig B, Hattori K, Friedrich M, Rafii S, Werb Z. Angiogenesis: vascular remodeling of the extracellular matrix involves metallo-proteinases. Curr Opin Hematol 2003; 10: 136–141.

20 Lyden D, Hattori K, Dias S, Costa C, Blaikie P, Butros L et al. Impaired recruitment of bone-marrow-derived endothelial and hematopoietic precursor cells blocks tumor angiogenesis and growth. Nat Med 2001; 7: 1194–1201.

21 Heissig B, Rafii S, Akiyama H, Ohki Y, Sato Y, Rafael T et al. Low-dose irradiation promotes tissue revascularization through VEGF release from mast cells and MMP-9-mediated progenitor cell mobilization. J Exp Med 2005; 202: 739–750.

22 Heissig B, Hattori K, Dias S, Friedrich M, Ferris B, Hackett NR et al. Recruitment of stem and progenitor cells from the bone marrow niche requires MMP-9 mediated release of kit-ligand. Cell 2002; 109: 625–637.

23 Doussis-Anagnostopoulou IA, Talks KL, Turley H, Debnam P, Tan DC, Mariatos G et al. Vascular endothelial growth factor (VEGF) is expressed by neoplastic Hodgkin-Reed-Sternberg cells in Hodgkin's disease. J Pathol 2002; 197: 677–683.

24 Rafii S, Lyden D, Benezra R, Hattori K, Heissig B. Vascular and haematopoietic stem cells: novel targets for anti-angiogenesis therapy? Nat Rev Cancer 2002; 2: 826–835.

25 Kaplan RN, Riba RD, Zacharoulis S, Bramley AH, Vincent L, Costa C et al. VEGFR1-positive haematopoietic bone marrow progenitors initiate the pre-metastatic niche. Nature 2005; 438: 820–827.

26 Lenz G, Wright G, Dave SS, Xiao W, Powell J, Zhao H et al. Stromal gene signatures in large-B-cell lymphomas. N Engl J Med 2008; 359: 2313–2323.

27 Okada Y, Gonoji Y, Naka K, Tomita K, Nakanishi I, Iwata K et al. Matrix metalloproteinase 9 (92-kDa gelatinase/type IV collage-nase) from HT 1080 human fibrosarcoma cells. Purification and activation of the precursor and enzymic properties. J Biol Chem 1992; 267: 21712–21719.

28 Suzuki K, Enghild JJ, Morodomi T, Salvesen G, Nagase H. Mechanisms of activation of tissue procollagenase by matrix metalloproteinase 3 (stromelysin). Biochemistry 1990; 29: 10261–10270.

29 Lyons RM, Keski-Oja J, Moses HL. Proteolytic activation of latent transforming growth factor-beta from fibroblast-conditioned medium. J Cell Biol 1988; 106: 1659–1665.

30 Roy JS, Van Themsche C, Demers M, Opdenakker G, Arnold B, St-Pierre Y. Triggering of T-cell leukemia and dissemination of T-cell lymphoma in MMP-9-deficient mice. Leukemia 2007; 21: 2506–2511.

31 Palumbo JS, Talmage KE, Liu H, La Jeunesse CM, Witte DP, Degen JL. Plasminogen supports tumor growth through a fibrinogen-dependent mechanism linked to vascular patency. Blood 2003; 102: 2819–2827.

32 de Jong D, Enblad G. Inflammatory cells and immune micro-environment in malignant lymphoma. J Intern Med 2008; 264: 528–536.

33 Moons L, Shi C, Ploplis V, Plow E, Haber E, Collen D et al. Reduced transplant arteriosclerosis in plasminogen-deficient mice. J Clin Invest 1998; 102: 1788–1797.

34 Lukacs N, Strieter R, Lincoln P, Brownell E, Pullen D, Schock H et al. Stem cell factor (c-kit ligand) influences eosinophil recruitment and histamine levels in allergic airway inflammation. J Immunol 1996; 156: 3945–3951.

35 Ferland C, Guilbert M, Davoine F, Flamand N, Chakir J, Laviolette M. Eotaxin promotes eosinophil transmigration via the activation of the plasminogen-plasmin system. J Leukoc Biol 2001; 69: 772–778.

36 Martinelli-Klay CP, Mendis BR, Lombardi T. Eosinophils and oral squamous cell carcinoma: a short review. J Oncol 2009; 2009: 310132.

37 Reimann M, Lee S, Loddenkemper C, Dorr JR, Tabor V, Aichele P et al. Tumor stroma-derived TGF-beta limits myc-driven lympho-magenesis via Suv39h1-dependent senescence. Cancer Cell 2010; 17: 262–272.

38 Lin EY, Nguyen AV, Russell RG, Pollard JW. Colony-stimulating factor 1 promotes progression of mammary tumors to malignancy. J Exp Med 2001; 193: 727–740.

Supplementary Information accompanies the paper on the Leukemia website (http://www.nature.com/leu)

IMMUNOBIOLOGY

Brief report

Imatinib mesylate directly impairs class switch recombination through down-regulation of AID: its potential efficacy as an AID suppressor

*Toyotaka Kawamata,[1] *Jun Lu,[2] *Tadayuki Sato,[3] Masafumi Tanaka,[4] Hitoshi Nagaoka,[5] Yasutoshi Agata,[6] Takae Toyoshima,[2] Kazuaki Yokoyama,[1] Naoki Oyaizu,[7] Naoya Nakamura,[8] Kiyoshi Ando,[9] †Arinobu Tojo,[1] and †Ai Kotani[2]

[1]Department of Hematology-Oncology/Molecular Therapy, Institute of Medical Science, University of Tokyo, Tokyo, Japan; [2]Institute of Innovation Science and Technology, Tokai University, Kanagawa, Japan; [3]Center for Education and Support, Department of Medicine, Tokai University, Kanagawa, Japan; [4]Molecular Life Science, Department of Medicine, Tokai University, Kanagawa, Japan; [5]Molecular Pathology, Department of Medicine, Gifu University, Gifu, Japan; [6]Immunology, Department of Medicine, Kyoto University, Kyoto, Japan; [7]Department of Laboratory Medicine in Research Hospital, Institute of Medical Science, University of Tokyo, Tokyo, Japan; [8]Pathology, School of Medicine, Tokai University, Kanagawa, Japan; and [9]Hematology and Oncology, School of Medicine, Tokai University, Kanagawa, Japan

Activation-induced cytidine deaminase (AID) is essential for class switch recombination and somatic hypermutation. Its deregulated expression acts as a genomic mutator that can contribute to the development of various malignancies. During treatment with imatinib mesylate (IM), patients with chronic myeloid leukemia often develop hypogammaglobulinemia, the mechanism of which has not yet been clarified. Here, we provide evidence that class switch recombination on B-cell activation is apparently inhibited by IM through down-regulation of AID. Furthermore, expression of E2A, a key transcription factor for AID induction, was markedly suppressed by IM. These results elucidate not only the underlying mechanism of IM-induced hypogammaglobulinemia but also its potential efficacy as an AID suppressor. (*Blood.* 2012;119(13): 3123-3127)

Introduction

Activation-induced cytidine deaminase (AID) is essential for class switch recombination (CSR) and somatic hypermutation.[1] Deregulated expression of AID acts as a genomic mutator and can contribute to tumorigenesis through genomic recombination and aberrant somatic hypermutation.[2-4] E2A, which harbors 2 binding sites in the AID promoter, is the crucial transcription factor for induction of AID.[5] Imatinib mesylate (IM) has diverse immunomodulatory effects,[6,7] including reduction of T-cell proliferation and inhibition of T-cell effector functions.[8,9] Previously, we reported that serum titers of IgG and IgA, but not IgM, were significantly lower in chronic myeloid leukemia patients treated with IM versus those treated with IFN-α,[10] suggesting that IM impairs CSR. In the present study, we investigated the effects of IM on CSR both in vitro and in vivo. Here, we present evidence that IM inhibits CSR through down-regulation of AID expression in splenic B cells.

Methods

Mouse immunization

Eight-week-old mice were immunized as previously reported,[1] with or without 50 mg/kg imatinib mesylate. The experiments were approved by the Committee of Animal Care at the Institute of Medical Science, University of Tokyo.

Immunohistochemistry

Immunostaining for AID was performed on frozen sections following the manufacturer's instructions using an AID antibody (H-80; Santa Cruz Biotechnology).

Primer sequences, reagents, and more detailed methods are shown in supplemental Methods (available on the *Blood* Web site; see the Supplemental Materials link at the top of the online article).

Results and discussion

CSR is induced in splenic B cells by stimulation with IL-4 and lipopolysaccharide (LPS).[11] After stimulation with IL-4 and LPS for 72 hours, IM decreased the proportion of IgG1-positive B cells dose-dependently. The proportion of B cells expressing surface IgG1 was approximately 16% without IM but was significantly reduced to approximately 3% with 10μM IM (Figure 1A). In the present culture system, only B cells can survive and proliferate,[1] suggesting that IM may act directly on B cells and inhibit their CSR.

Next, we examined expression of the germline transcript directed by the I promoter of IgG1 and AID, both of which are essential for CSR after B-cell stimulation.[12] Expression of AID was suppressed by IM dose-dependently (Figure 1B), whereas the IgG1 germline transcripts were not decreased by IM (Figure 1C). Likewise, IgA CSR in CH12F3-2A cells was impaired by IM in a dose-dependent manner (Figure 1D). These results

The online version of this article contains a data supplement.